UNITED STATES DEPARTMENT OF THE INTERIOR

GEOLOGICAL SURVEY

Dissolution of Sphalerite in Ferric Chloride Solution

By

Huai Su

Open-File Report 81-609

1981

This report has not been edited for conformity with Geological Survey editorial standards or stratigraphic nomenclature

CONTENTS

ILLUSTRATIONS

TABLES

Dissolution of sphalerite in ferric chloride solution

By Huai Su

ABSTRACT

The dissolution of sphalerite in acidic ferric chloride solution of polished flat surfaces and of spherical particle surface was investigated. Tests were conducted on sphalerite to study rate of dissolution by the effects of stirring speed, temperature, ferric and ferrous concentrations, purity, and particle size.

Kinetic investigations were conducted in a nitrogen atmosphere with temperature ranges of 44°C to 90°C. The activation energy for the dissolution process is -11.2 $\pm$ 2.7 Kcal per mole.

The kinetics show chemical reaction as being important at the initial stages of leaching, and ion diffusion through a product layer as being important during the later stages of reaction. The mixed-control equation is an excellent description of the rate of dissolution of a sphalerite particle.

$$K_r t = 1 - (1-R)^{1/3} + B\,[1 - 2/3\ R - (1-R)^{2/3}]$$

where K_r = dissolution rate, $min.^{-1}$, t = leaching time, minutes, R = fraction of sphalerite converted, %, B = constant for mixed-control model.

The basic kinetic data of this investigation could be applicable to engineering design of the leaching process.

INTRODUCTION

Direct leaching of sphalerite and other sulfides with ferric ions has been extensively studied (Dutrizac and MacDonald, 1974). Ferric sulfate and ferric chloride are two of the most important leaching reagents for supplying ferric ions. Ferric sulfate reagent is naturally occurring and cheaply produced; ferric chloride has been tested frequently and was recognized to be stronger than ferric sulfate (Jones and Peters, 1976).

Brown and Sullivan (1934) reported that ferric chloride is a better leaching agent than ferric sulfate in the dissolution of chalcopyrite concentrate. At 100°C, 18 percent of the copper was extracted in 3 hours by a 5 percent ferric chloride solution, whereas only 4 percent copper extraction was achieved by an equivalent ferric sulfate solution under the same conditions. Haver and Wong (1971) studied the dissolution of chalcopyrite concentrate by concentrated acidified ferric chloride solutions. At 106°C, copper extractions in excess of 99 percent were achieved within 2 hours. Parabolic kinetics were reported and was attributed to mass transfer during the leaching of ferric ions through the

constantly thickening sulfur layer. Ferric chloride leaching studies have also been successfully conducted on stibnite (Sb_2S_3) by Tugov and Tsyganov (1965), on tetrahedrite by Carey (1971), and on galena by Murray (1972).

The dissolution of sphalerite or zinc sulfide by ferric ions in the temperature interval 80°C to 100°C was studied by Kuzminkh and Yakhontova (1951). The overall reaction is:

$$ZnS + 2Fe(III) = Zn(II) + 2Fe(II) + S^{o} \quad (1)$$

The initial dissolution rate was directly proportional to the concentration of ferric ion. The rate increased with increasing ferric ion concentration to a maximum of two to three times the stoichiometric requirement. Therefore, additional increase in ferric ion concentration did not affect the rate. The overall kinetics and rate-controlling process appeared to be diffusion of ferric ions.

Ablanov and others (1961) and Ermilov (1961) reported that with production of elemental sulfur sphalerite was readily soluble in acidic ferric chloride solutions. Ermilov's results showed that a 150-percent theoretical excess of an acidic ferric chloride solution containing 100 g/l ferric ions and 50 g/l ferrous ions could extract more than 85 percent of the zinc from a sphalerite-bearing pyrite ore.

Zapevalov and Vygoda (1964) found that zinc sulfide could be readily leached from matte in 1-2 hours at 100°C using solutions containing 50 to 100 g/l $FeCl_3$. The addition of xylene to the ferric chloride leaching solution permitted the simultaneous extractions of the elemental sulfur formed during leaching. A 20 to 30 percent excess of ferric ions was desirable.

The foregoing discussion shows that sphalerite can be readily dissolved under certain conditions (Beckstead and others, 1976; and Jan and others, 1976). However, few kinetic studies of sphalerite dissolution are reported. The objectives of these investigations were:

1. To study the important factors involved in the leaching of sphalerite by ferric chloride, such as temperature, ferric ion concentration, particle size, impurities, and stirring rate.
2. To ascertain whether the rate-determining step is the diffusion of ferric ion or products through the porous sulfur layer, the chemical reaction at the liquid-solid interface, or a combination of these rate-determining steps.

Acknowledgements.--The author thanks Professors Gene E. Bobeck and C. M. Wai of University of Idaho for their critical reviews for this report.

STRUCTURE AND PROPERTIES OF SPHALERITE

In sphalerite crystals the bonding is predominantly covalent where two elements, Zn and S, form tetrahedrally distributed orbitals of the hybrid sp^3 type. The structure can be compared to two interpenetrating face-centered cubic lattices with sulfur atoms centering on the points of one and zinc atoms on the other. Each zinc atom is bonded by electron pairs to each of four sulfur atoms, and each sulfur atom is in turn bonded to four neighboring zinc atoms (fig. 1). The ratio of valence electrons to atoms is 4:1. This ratio favors the stability of the tetrahedrally coordinated sphalerite structure (Bloss, 1971).

Sphalerite, as it occurs in nature, varies widely in color and appearance, depending on the identity and amount of impurities present. Color ranges from white in the pure state to yellowish brown to deep black as the amount of iron increases. Marmatite, (Zn,Fe)S, contains up to 20 percent of iron and is dark brown to black. The specific gravity of sphalerite is about 4.0 to 4.1. The composition of pure sphalerite is 67 weight percent zinc and 33 weight percent sulfur. In nature, sphalerite always contains iron which occupies the sites of zinc ions in the lattice. Manganese and cadmium are usually present in small amounts in solid solution.

Sphalerite, the most common mineral of zinc, is found in contact metamorphic deposits where the sulfide ores have been derived from an igneous intrusion and deposited by replacement in adjacent rock. It is also found in veins in eruptive and sedimentary rocks. Of the two types of zinc sulfide, sphalerite is the one which is formed below 1,020°C, and wurtzite is the stable one formed at higher temperatures. The difference between the wurtzite and sphalerite structures lies in the arrangement of the sulfur atoms, which in wurtzite corresponds to a hexagonal close-packing of spheres and in sphalerite corresponds to a cubic close-packing of spheres.

PHYSICAL CHEMISTRY CONSIDERATION

Thermodynamics

The standard free energy (8, 19), $\Delta G°$, change for the reaction (1) between sphalerite and ferric chloride solution at 25°C can be calculated as follows:

$$ZnS\ (s) + 2Fe\ (III)\ (aq) = Zn(II) + 2Fe(II)\ (ag) + S^{o}\ (s)$$

$$\Delta G° = -97.88 + 2(-81.59) + 0 - (-48.11) - 2\ (-95.2) = -22.6\ \text{Kcal/mole}$$

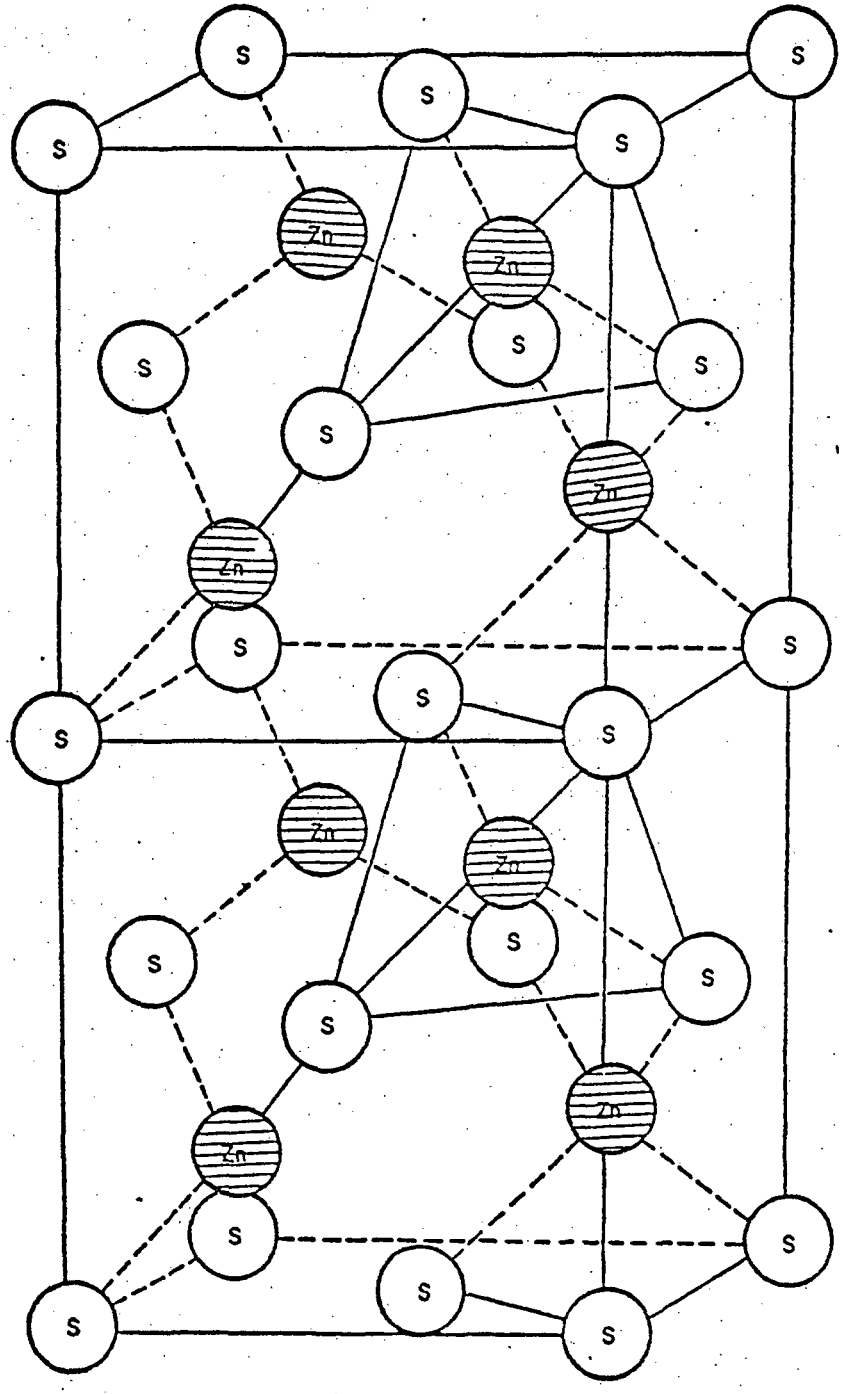

FIGURE 1.--DIAGRAM SHOWING TWO UNIT-CELL IN THE STRUCTION OF SPHALERITE. IN EACH UNIT, EACH ZINC ATOM IS BONDED BY ELECTRON PAIRS TO EACH OF FOUR SULFUR ATOMS.

The reaction will be thermodynamically possible from left to right, because the value of the free energy change is negative. The equilibrium constant, K, can be calculated according to the following relationship

$$\triangle G^\circ = RT \ln K \qquad (2)$$

where $K = (a_{Fe^{++}})^2 (a_{Zn^{++}}) (a_{S^\circ}) / (a_{Fe^{+++}})^2 (a_{ZnS})$

and "a" is activity.

The activities of sulfur and sphalerite are taken as unity. The equilibrium constant, K, calculated with the use of Equation (2), is about 10^{16}. An equilibrium constant of this magnitude indicates that reaction (1) should be nearly complete at 25°C for any significant concentration of Fe (III). The rapidity of the reaction is a kinetic problem discussed later in this report.

Electrochemical Reactions

The leaching of sphalerite in acidified ferric ion solution can also be expressed in terms of oxidation-reduction half-cell reactions. Reactions occur at the anodic side (Latimer, 1952):

$$Zn + S^{--} = ZnS + 2e^- \qquad E^\circ = 1.44 \text{ volts}$$

$$Zn^{++} + 2e^- = Zn \qquad E^\circ = -0.763 \text{ volts}$$

$$+ \quad S^\circ + 2e^- = S \qquad E^\circ = -0.48 \text{ volts}$$

$$S^\circ + Zn^{++} + 2e^- = ZnS \qquad E^\circ = 0.197 \text{ volts}$$

or $ZnS = Zn^{++} + 2e^- + S^\circ \qquad E^\circ_{red.} = -0.197$ volts

Reactions occur at the cathodic side:

$$2Fe^{+++} + 2e^- = 2Fe^{++} \qquad E^\circ_{ox.} = 0.771 \text{ volts}$$

For the reaction between ZnS and Fe^{+++} the overall electrode potential is obtained as follows:

$$E^\circ_{all} = E^\circ_{ox.} + E^\circ_{red.} = 0.574 \text{ volts/mole}$$

A change in electrode potential, E°, results in a change in the free energy, $\triangle G^\circ$, of reaction by nFE° per mole, where F is the Faraday constant and n is the number of electrons transferred. If the concentration of ions involved in the electrode reaction is assumed to be at unit activity, then the equation is:

$$\triangle G^\circ = -nfE^\circ = -23060 \times 2 \times 0.574 = -26.5 \text{ kcal/mole}$$

This value is close to the value, -22.6 kcal/mole, which was calculated from the free energy change for reaction (1).

Pourbaix Diagram

The leaching of sulfides is similar to the corrosion process in which the reaction of a sulfide with its environment results in the continuing destruction of the sulfide. Pourbaix (1966) developed a graphical means for displaying the domain of phase stability in terms of voltage and pH for each species in a leaching system at fixed composition. Changes in the concentration of the constituents cause shifts in the positions of the lines in the diagrams.

The derivation of Eh-pH diagrams is based on the general reduction equation in aqueous solution (Wadsworth and Malouf, 1972a):

$$aA + bB + mH^{+} + ne^{-} = cC + dD \qquad (3)$$

where A = oxidized species

C = reduced species

B & D = auxiliary species or water

The electrode potential for Equation (3) can be written:

$$Eh = E^{\circ} - \frac{2.3RT}{nf}(m/n)\,pH - \frac{2.3RT}{nf}\log(a_C^c a_D^d / a_A^a a_B^b) \qquad (4)$$

where f is the Faraday constant.

On the diagram, the slope is proportional to $(-\frac{m}{n})$. Thus, when "m" is zero, the line is horizontal; when "n" is zero, the line is vertical.

Figure 2 shows the Zn-H_2O-Fe-S system. This diagram is based on the concentrations used in the present leaching experiments. The concentration of iron is 0.25 molar and of zinc ion, 0.05 molar. This diagram is incomplete but indicates the most important domains in which the species at 25° at a given Eh and pH are thermodynamically stable.

The diagram graphically describes which pH values could result in the precipitation of certain species. The pH can thus be controlled during subsequent leaching experiments. The numbers in parentheses on lines in figure 2 correspond to the chemical reaction equation number shown in "Calculation of Eh-ph diagram of sphalerite." For example: lines (1) and (2) in figure 2 indicate that water is stable only within certain limits of oxidation or reduction potential, oxygen or hydrogen being evolved when these are exceeded. The upper limit of water stability can be calculated on the basis of the reaction

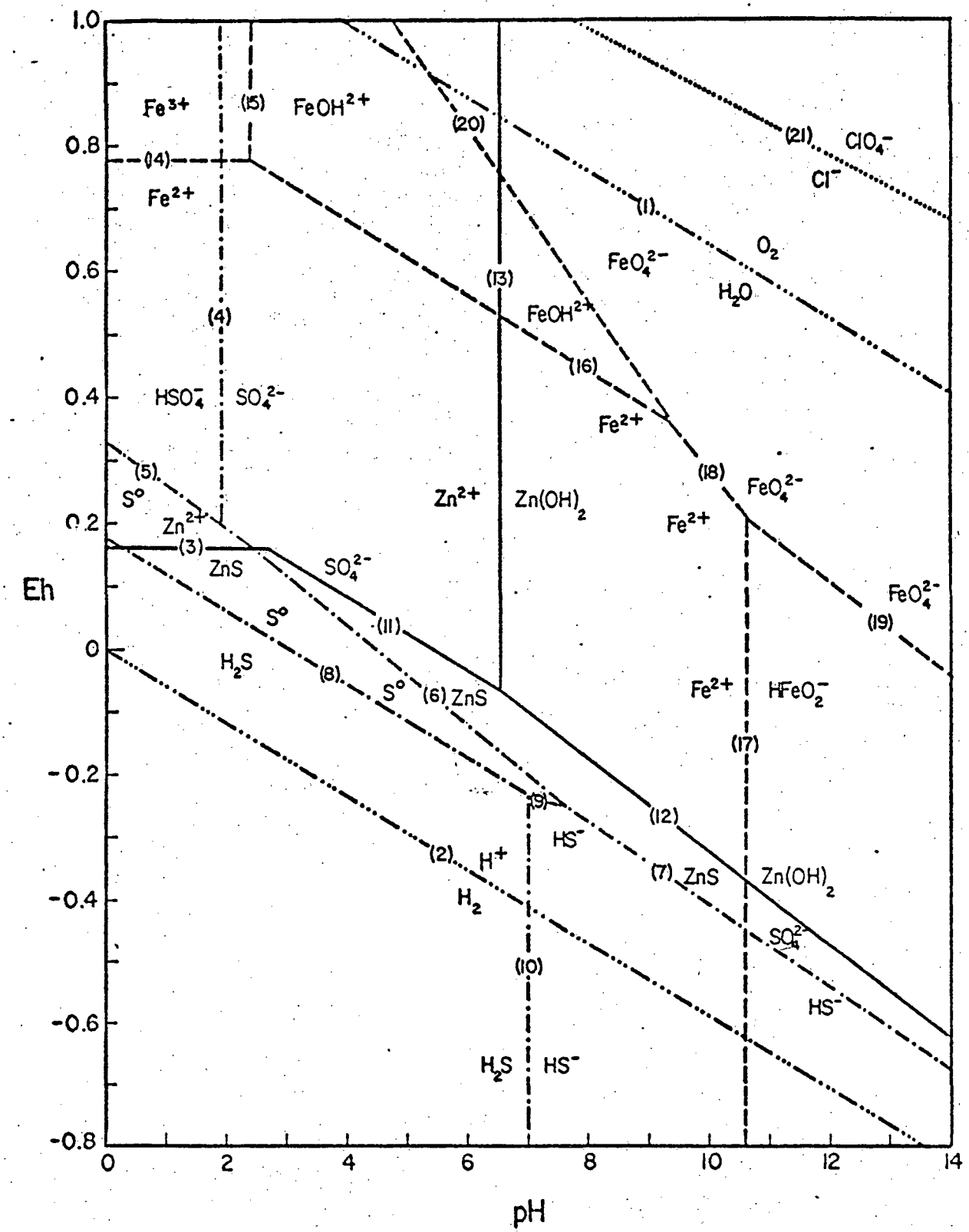

FIGURE 2.--DIAGRAM SHOWING SPHALERITE IN AQUEOUS SOLUTION.

$$2H_2O = O_2 + 4H^+ + 4e^- \qquad \text{at } 25°C$$

and $$Eh = 1.23 + \frac{0.059}{4} \log (H^+)^4 (P_{O_2}) \text{ with } E° = 1.23 \text{ volts}$$

Assume $P_{O_2} = 1$ atm, then

$$Eh = 1.23 = 0.059 \text{ pH}.$$

The lower limit of water stability if obtained similarly by using the half-cell reaction

$$2H^+ + 2e^- = H_2 \qquad E° = 0$$

Thus $$Eh = 0 + \frac{0.059}{2} \log(H^+)^2 = 0 - 0.059 \text{ pH}$$

When ZnS leaches in the presence of Fe(III) ion solution under acidic and oxidizing conditions, elemental sulfur will be formed. Further, sulfur will be oxidized to sulfate according to the reaction, $S° + 4H_2O = SO_4^{--} + 6e^- + 8H^+$ (line 6). But under non-oxidizing conditions the elemental sulfur will become H_2S according to the reaction, $H_2S = S°\ (c) + 2H^+ + 2e^-$ (line 8). Sulfur is also unstable in the presence of alkaline solutions in which it tends to form HS^- and SO_4^{--} (fig. 2). Hence the stability domain of sulfur enclosed by lines (5), (6), (9), and (8), is roughly triangular and very narrow.

The stability domain of ferric ion is also in the acidic region. The boundary line (15) between Fe^{+++} and $FeOH^{++}$ in figure 2 is according to the reaction, $Fe^{+++} + H_2O = FeOH^{++} + H^+$. The $FeOH^{++}$ will deposit as Fe_2O_3 as the pH of solution is raised to 2.4 ($2FeOH^{++} + H_2O = Fe_2O_3 + 4H^+$). The precipitation of Fe_2O_3 is undesirable in the leaching system. The pH of the solution must be kept below 2.4 if precipitation of Fe_2O_3 is to be avoided.

Zinc ion is stable between pH range 0 to 6.6 as shown on boundary line (13). Above pH 6.6 it precipitates as $Zn(OH)_2$. The system will naturally assume interparticle potentials in the range of stability of all ions Zn^{++}, Fe^{+++}, Fe^{++}, and $S°$.

REVIEW OF KINETIC MODEL

The dissolution of zinc sulfide particles in acidified ferric chloride solution is assumed to be a heterogeneous process involving mass transport of ferric ions, ferrous ions and zinc ions, and one or more interface reactions. The reaction is irreversible thermodynamically and it proceeds in a topochemical manner. That is, as the reaction continues, a progressively thicker outer shell of elemental sulfur is formed, while the inner core of unreacted sulfide decreases. Diffusion of ferric ion and ferrous ion through

the porous sulfur layer is required for continued reaction. The solid product sulfur layer is assumed to be of uniform thickness from point to point over the surface of the particle. The thickness of sulfur is directly proportional to the quantity of zinc ions which have been produced.

The overall reaction process may be broken down into steps, some of which are as follows (figure 3):

1. Transport of reactant, ferric ion, Fe(III), through the liquid film surrounding the particle to the surface of the solid.
2. Diffusion of ferric ions through the liquid contained in the pores of the product sulfur layer to the ZnS/S interface.
3. Chemical reaction at the liquid-zinc sulfide or S/ZnS interface which results in consumption of Fe(III) ion and generation of sulfur and Fe(II) ion; at the same time the ZnS core is consumed. Chemical reaction at the sulfur-zinc sulfide interface may include steps of adsorption, electron-transfer reaction, and desorption.
4. Diffusion of soluble products of the reaction, Fe(II) and Zn(II), through the porous sulfur layer (Bartlett, 1972).
5. Transport of soluble products away from the solid-liquid interface.

The five main steps shown above occur in series and each offers some resistance to the overall rate of the process. Thus, their effects are additive, in analogy with the additive nature of electrical resistances in series. If the resistance offered by one step happens to be much greater than the sum of the other steps, then that corresponding step is said to be the rate-controlling step. The relative importance of these various steps may change continuously during the reaction for any given conditions. At times, some of these steps do not exist. For example, when the stirring rate was rapid enough to reduce the thickness of the stagnant liquid film surrounding the particle to a minimum, the contribution of steps (1) and (5) are minimized.

The five steps may be described mathematically with the following assumptions (Levenspiel, 1972):

(1) The particle is assumed to be spherical and it retains its original dimensions during the entire dissolution process.
(2) The reaction proceeds spherical-symmetrically and irreversibly.
(3) The fluid-solid reactions are noncatalytic reactions.
(4) The reaction occurs in a pseudo-steady-state condition over any small period of time, i.e., the three rates--diffusion of ferric

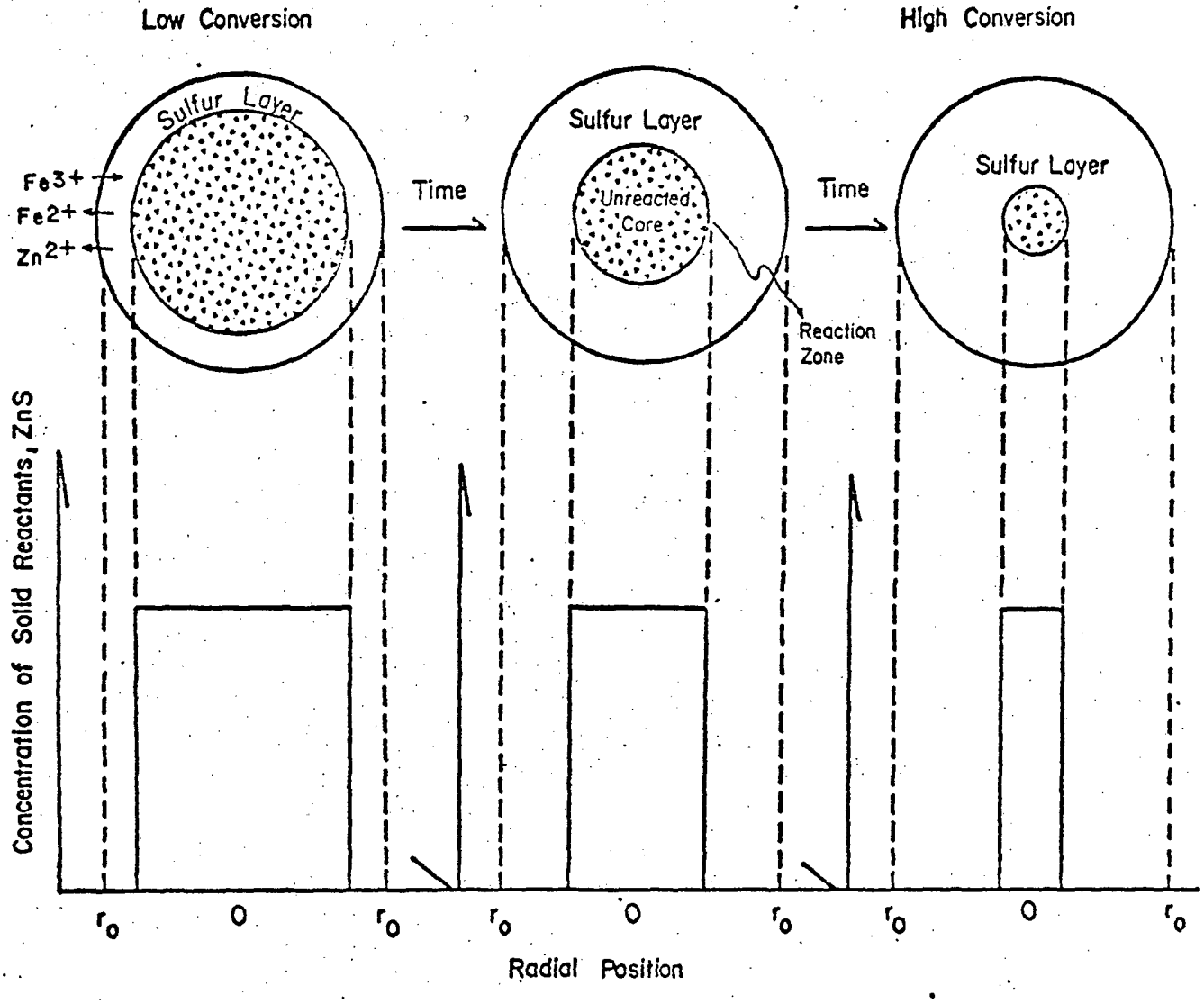

FIGURE 3.--DIAGRAM SHOWING SPHALERITE PARTICLE REACTION. REACTION PROCEEDS AT THE OUTER SKIN OF THE PARTICLES. THE ZONE OF REACTION THEN MOVES INTO THE SOLID PARTICLE.

ion through the liquid film, diffusion through the sulfur layer, and reaction at interface--are identical.

As previously mentioned, the overall reaction involves mass transfer across the liquid boundary layer, transport across the sulfur layer, and chemical reaction at the interface. Three models for mathematical rate expressions are now summarized under the rapid stirring condition:

1. Model Based on Control of Reaction Rate by Rate of Diffusion Through Sulfur Layer (Levenspiel, 1972).

The dissolution of sphalerite in acidic ferric chloride solution, produces sulfur which forms on the surface of a particle. The sulfur layer is porous, permitting the diffusion of ions to the particle surface. The kinetics are controlled by the transport of ferric ion and products of zinc or ferrous ions through the porous sulfur layer. The rate expression is derived as (5):

$$K_p t = 1 - \frac{2}{3}R - (1-R)^{2/3}$$

where

$$Kp = \frac{2bMD_eC_{fs}}{r_o^2 Pz}$$

$$R = \text{fraction reacted} = 1 - \frac{\text{volume of unreacted core}}{\text{original volume of particle}}$$

$$= 1 - (\tfrac{4}{3}\pi r_c^3) / (\tfrac{4}{3}\pi r_o^3)$$

$$= 1 - \left(\frac{r_c}{r_o}\right)^3$$

r_o: Radius, of original particles, cm

r_c: ZnS core radius, cm

C_{fs}: Concentration of Fe^{+++} ion in sulfur layer or mineral surface

b: Stoichiometric Coefficient

D_e: Effective diffusion coefficient of ions in porous medium, cm^2/min

K_p: Parabolic rate, min^{-1}

M: Molecular weight of the particular sulfide mineral

P_z: Density of sphalerite

t: Time, min

2. Model Based on Control of Reaction Rate by Rate of Chemical Reaction (Levenspiel, 1972)

In this model, the rate of consumption of reactants, Fe(III), and formation of product sulfur layer are proportional to the area of the unreacted core of the particle. The progress of reaction is unaffected by the presence of any product layer. The rate expression may be written as:

$$K_c t = 1 - (1-R)^{1/3} \qquad (6)$$

where

$K_c = \frac{MbK_{cc}C_{fc}}{p_z r_o}$ with the dimension t^{-1}

K_{cc}: Chemical rate constant

C_{fc}: Concentration of Fe^{+++} ion at unreacted particle core

K_c: Chemical linear rate, min^{-1}

3. Model Based on Control of Reaction Rate by Both Rate of Diffusion and Rate of Chemical Reaction.

Equations (5) and (6) were developed on the assumption that a single resistance controls the rate of dissolution of a particle throughout the course of the process. However, the relative importance of the liquid film, the sulfur layer and the interface steps may vary as the reaction progresses. In general, then, it may not be reasonable to consider that just one step controls throughout the reaction.

A mixed-control equation (Cordell, 1968; Habashi, 1970; Levenspiel, 1972; Lu, 1963; Wadsworth and Malouf, 1972b; Wen, 1968) was derived assuming at the pseudo-steady state that the rate of chemical reaction at the interface is of equal magnitude to the rate of diffusion through the sulfur layer. The reaction rate will be expressed as:

$$\frac{MbK_{cc}D_e C_{fs}}{p_z r_o^2} t = \frac{Kcc}{2} \left[1 - \frac{2}{3} R - (1-R)^{2/3} + \frac{D_e}{r_o}\left(1 - (1-R)^{1/3}\right)\right] \qquad (7)$$

The equation shows that both the chemical reaction at the surface of a particle and mass transport of ferric ion through the sulfur layer contribute to the overall rate during the reaction.

EXPERIMENTAL APPARATUS AND PROCEDURE

The leaching experiments were conducted in the reaction flask at temperatures ranging from 44°C to 90°C. The equipment was maintained at a constant temperature which permitted the withdrawal of solution samples at defined intervals.

The samples tested were sphalerite flotation concentrates obtained from St. Joe Minerals (Balmat, New York), from U.V. Industries, Inc. (Utah), and from ASARCO (Colorado). Some experiments were conducted by using the polished surface of pure sphalerite crystals and ore samples which were cut to about the size of 1/2 inch x 1/2 inch x 1/2 inch.

The sphalerite concentrates were gray in color. They were screened and washed in acetone to remove slimes and then dried overnight for experimental work. Shown in table 1 is the assay of the sized fraction of the three zinc concentrates by Perkin-Elmer Model 303 atomic absorption.

Deionized, distilled water was used in all experiments. Concentrated (38%) hydrochloric acid was used to acidify the ferric chloride solutions. Reagentgrade ferric chloride hexahydrate ($FeCl_3.6H_20$) was used to compare the leaching solution.

The leaching apparatus consisted of a 1-liter Pyrex reaction flask (fig. 4). The flask was heated in an oil bath, the temperature of which was controlled within about $\pm$ 1.0°C. The reaction flask was fitted with a Pyrex glass lid that contained three circumferential, uniformly spaced, standard taper ports, and one centrally located, larger standard-taper port. One of the three ports was fitted with a reflux condenser which was used to keep to a minimum evaporation losses within the reaction flask. Another of the small ports accommodated a 0° to 110°C thermometer that measured the temperature within $\pm$ 1.0°C. This opening also served as the charging port for inserting the leach sample or as the sampling port for removing samples of the leach solution. The third small opening served as the inlet port for the flowing nitrogen gas atmosphere maintained over the system. The center port accommodates a glass impeller with Teflon paddles which extended down into the leach solution. The impeller was driven by a variable speed motor. The rate of revolution was estimated by means of a stroboscobe and was held to $\pm$ 15 rpm by the control on the variable speed motor.

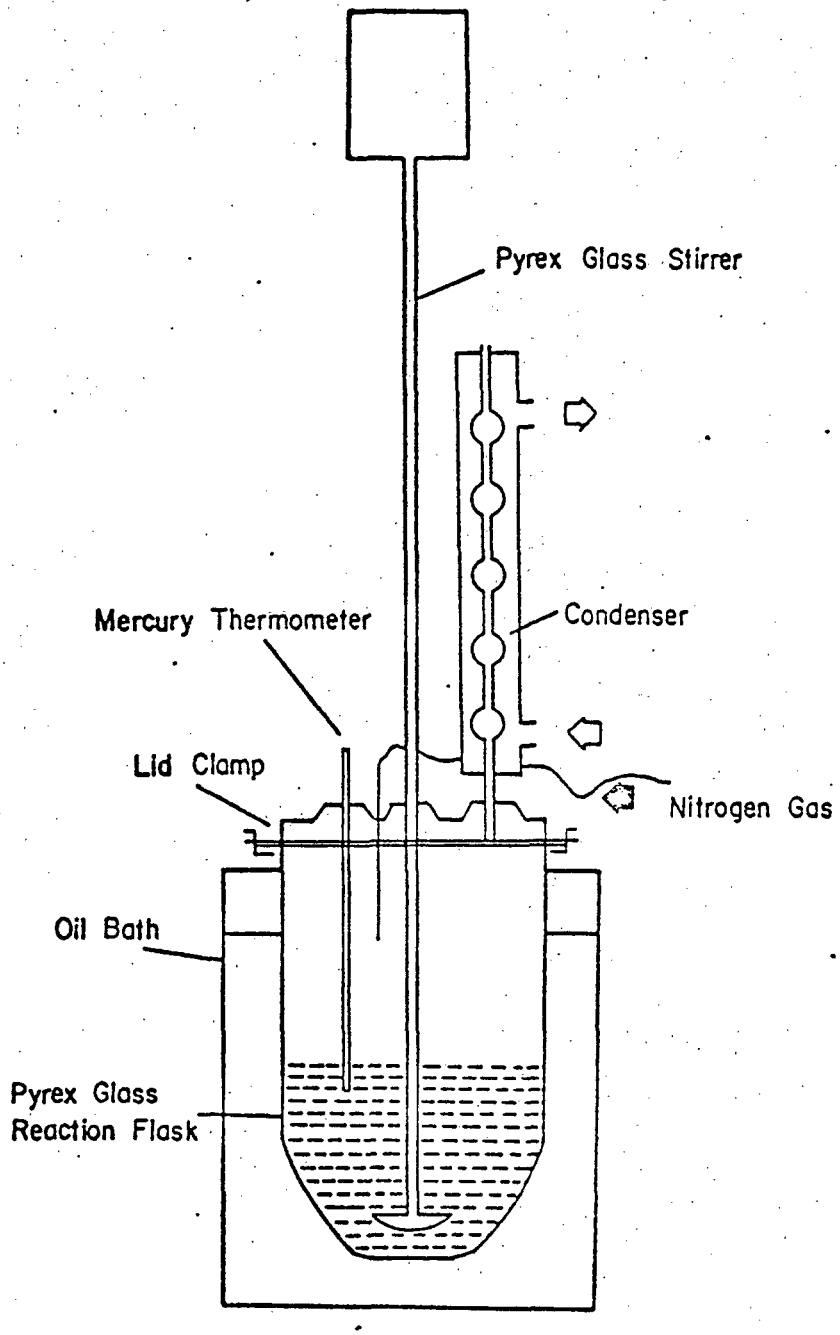

FIGURE 4.--A SCHEMATIC DIAGRAM OF THE LEACHING SYSTEM.

Table 1.--Chemical analysis of zinc concentrate

(-100 + 150 mesh), wt%

	Zn	Fe	Cu	Pb	Ca	Cd	Ag	Sb	Mg	
(1)	61.500	5.170	0.130	0.450	0.350	0.150	0.002	0.045	0.180	67.98
(2)	54.160	6.250	1.130	3.030	0.200	0.320	0.014	0.044	0.040	65.19
(3)	44.330	8.060	0.460	0.460	0.260	0.200	0.014	0.560	0.170	54.51

(1) St. Joe Minerals (Balmat, New York)
(2) U.V. Industries, Inc. (Utah)
(3) ASARCO (Colorado)

A standard leach procedure was followed:

(1) The concentrate was sized, acetone washed, and dried overnight. For sphalerite crystals it was mounted in a 1-inch Bakelite ring with epoxy, and polished for leaching tests.

(2) 500 ml of a known concentration of ferric chloride solution was placed in the 1-liter reaction flask; the pH of ferric chloride solution was kept below 2 by adding 20 ml of concentrated HCl per liter of solution before it was placed in the flask.

(3) The reaction flask was placed in the oil bath and heated to the desired temperature. A sample of concentrate of desired weight (1, 5, or 0.5 grams) was placed in a test tube and preheated in the oil bath. Prior to heating the reaction flask, nitrogen was bubbled through the solution for about 10 minutes. The flow of nitrogen was stopped during leaching to avoid temperature changes inside the flask.

(4) When the desired reaction temperature was reached, the preheated concentrate sample was put into the reaction flask and the mixture was stirred at the desired speed.

(5) Approximately 2 milliliters of solution was withdrawn with a pipet, during the experiment; 1 milliliter was used for chemical analysis, the other was set aside for rechecking the results. The time interval for sampling was about 10 to 60 minutes, depending on need. The calculation of concentrations of the sample solution was based on the volume of solution in the reaction flask at the time of the sample was withdrawn.

EXPERIMENTAL RESULTS AND DISCUSSION

Investigation was conducted to determine the rate of dissolution of sphalerite in acidified ferric chloride solution and the effects of the variables of temperature, particle size, ferric and ferrous ion concentration, agitation rate, and purity.

Stoichiometry of Chemical Reaction

The initial experiments were directed toward checking the stoichiometry of the leaching reaction (1). The results to be discussed are based on the experimental observations of the zinc concentrates supplied by St. Joe Minerals, Balmat, N.Y. The concentrates were leached in acidfied ferric chloride solutions at 87°C for various periods of time. The leaching was protected from oxidation by an atmosphere of nitrogen. Typical dissolved zinc and the formation of ferrous iron versus time curves are given in figure 5. The ordinate on the left side of figure 5 gives the concentration of zinc ion in solution at time, t, and the ordinate axis on the right gives the ferrous ion concentration converted at time t. The agreement between the two rate curves is good. The ratio of ferrous ion to zinc ion in the solution was approximately 2 (table 2). The products and their amounts were consistent with the following stoichiometry:

$$ZnS + 2Fe(III) \rightarrow Zn(II) + 2Fe(II) + S^{\circ} \qquad (1)$$

This confirms the results of other investigators (Dutrizac and MacDonald, 1974; Ermilov, 1960; Murray, 1972) who reported that a metal sulfide, immersed in an acidified ferric ion solution, often produces elemental sulfur and very little sulfate.

Murray (1972) studied and reported that both the galena (PbS) and sphalerite (ZnS) react with acidified ferric chloride solution producing elemental sulfur and the ratio of ferrous ion to metal element was approximately 2.

The microprobe analysis was also used to examine the sulfur layer growth allowing for leaching time for the leached flat surface of sphalerite crystal. The specimens were examined by simultaneous two-elements spectral scanning for S K_{α} and Zn K_{α} under the focused electron beam on the carbon surface of the specimen. Figure 6 shows the X-ray intensity across the sulfur layer profiles for Zn K_{α} and S K_{α} for three leached samples. The samples were leached 2 hours, 5 hours, and 8 hours, respectively, in 0.25 molar of ferric chloride solution at 70°C. Correspondingly, the thickness of sulfur layer is 0.8 microns, 5.6 microns, and 8.8 microns. The thickness of the sulfur layer (fig. 6) was

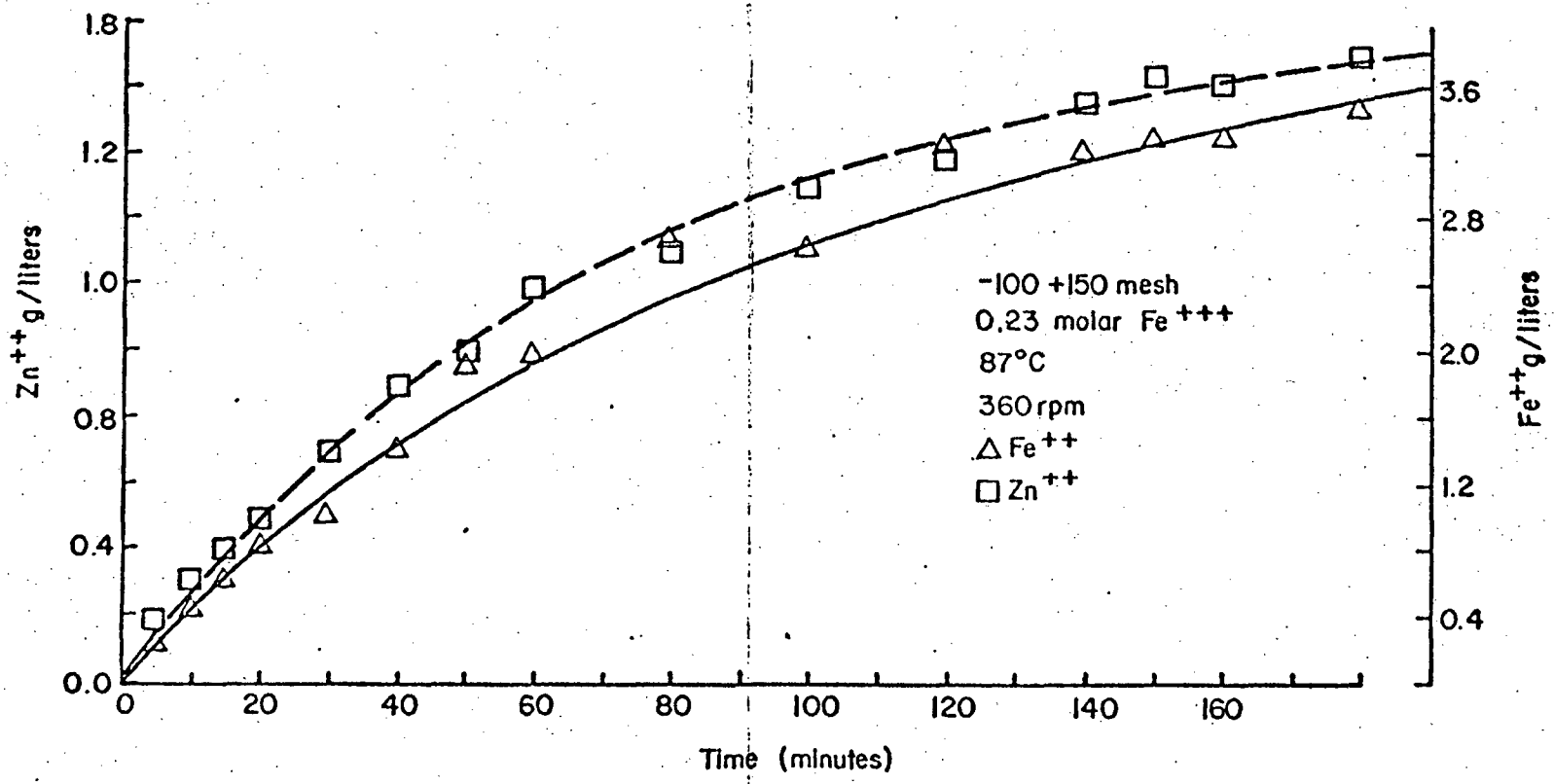

FIGURE 5.--PLOT SHOWING DISSOLUTION OF Z_NS AND FORMATION OF FERROUS IONS.

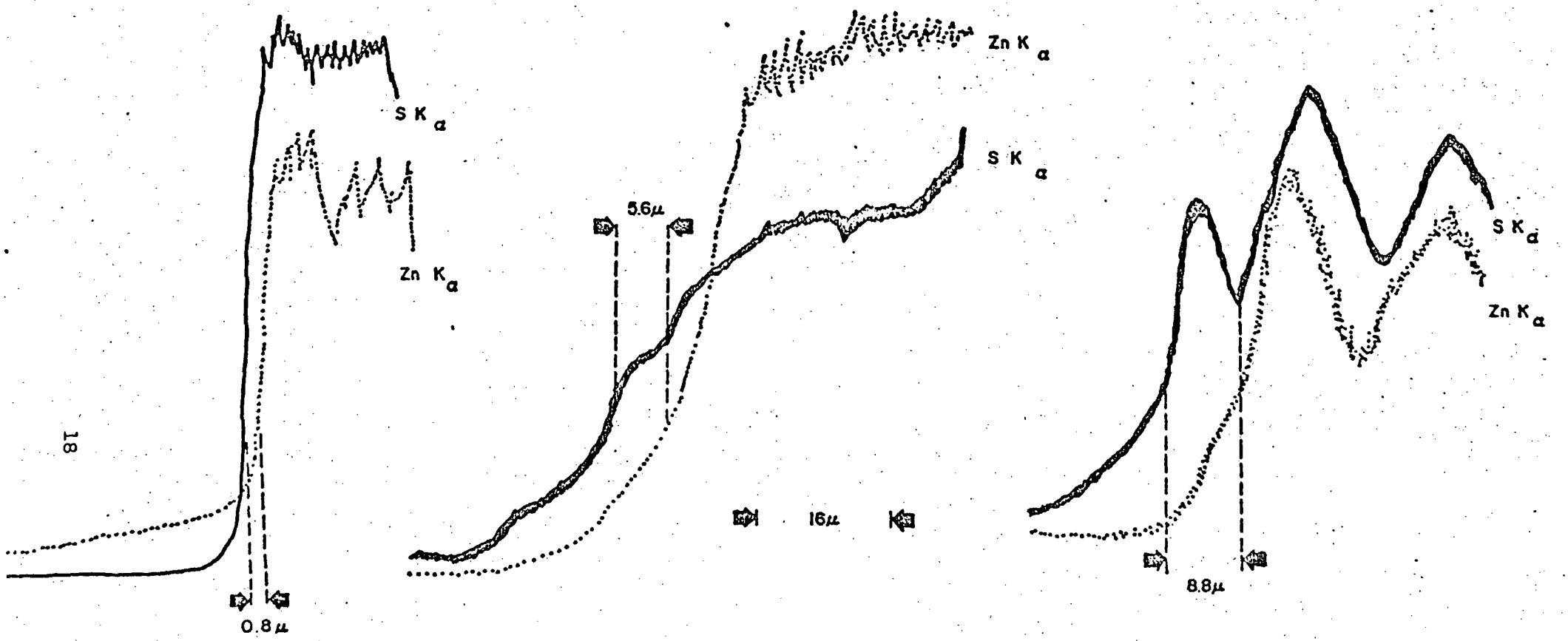

FIGURE 6.—SULFUR LAYER THICKNESSES FOR SAMPLES AFTER DIFFERENT LEACHING PERIODS, SHOWN ON X-RAY INTENSITIES.

measured by the gap between two X-ray profiles, S K_α and Zn K_α, with the scale of 16 microns per inch of chart paper. These two X-ray profile lines were scanned simultaneously across the sulfur layer by moving the sample 16 microns per minute which is equivalent to 1 inch on the chart paper. The moving stage is a calibrated motorized gear, operating at 16 microns per minute. The two points for measuring the thickness of the sulfur layer are chosen at the place where these two X-ray lines are roughly parallel, representing each of the two lines scanned over the specimen at the same spot and at the same time. The gap also includes the amount of offset of two pens, about 1/20 inch, which must be corrected in the thickness measurement. The thickness measurement is an approximated value, because it may contain errors on the position of spectrograph lines that are deviated due to the roughness of the sulfur surface. The peaks and valleys of the intensity profiles shown in figure 6 are also caused from roughness of the sulfur surface, that presumably was made during the preparation of the specimen. However, figure 6 is for demonstrating the sulfur layer growth with the leaching time. Accurate measurement of the sulfur-layer thickness was not required in this study.

Rate Dependence on Agitation

In the absence of agitation the dissolution reaction proceeds very slowly and appears to be controlled by liquid diffusion. Such a process follows the rate law controlled by mass transfer through the liquid boundary film.

$$\text{Rate} = \frac{D_e}{\delta'} \times A \times C_{fl} \qquad (8)$$

where

C_{fl} : Concentration of Fe^{+++} ion in solution

A : Area, cm^2

Inasmuch as the thickness of the liquid boundary, δ', decreases with increasing speed of stirring, the rate of dissolution increases as a consequence. Table 3 shows the results of a series of tests run at different stirring speed settings which are plotted in figure 7. At speeds below 300 rpm, a straight line was obtained by plotting the logarithm of rate constant, K_c, against the logarithm of speed of stirring. It is evident from figure 7 that the dissolution rate increases with increasing stirring rate up to about 300 rpm. At speeds below 300 rpm, Reaction (1) is controlled liquid-film diffusion and the rate can be usually expressed as a function of speed of stirring as follows:

$$\text{Rate of dissolution} \backsim (\text{rpm})^a$$

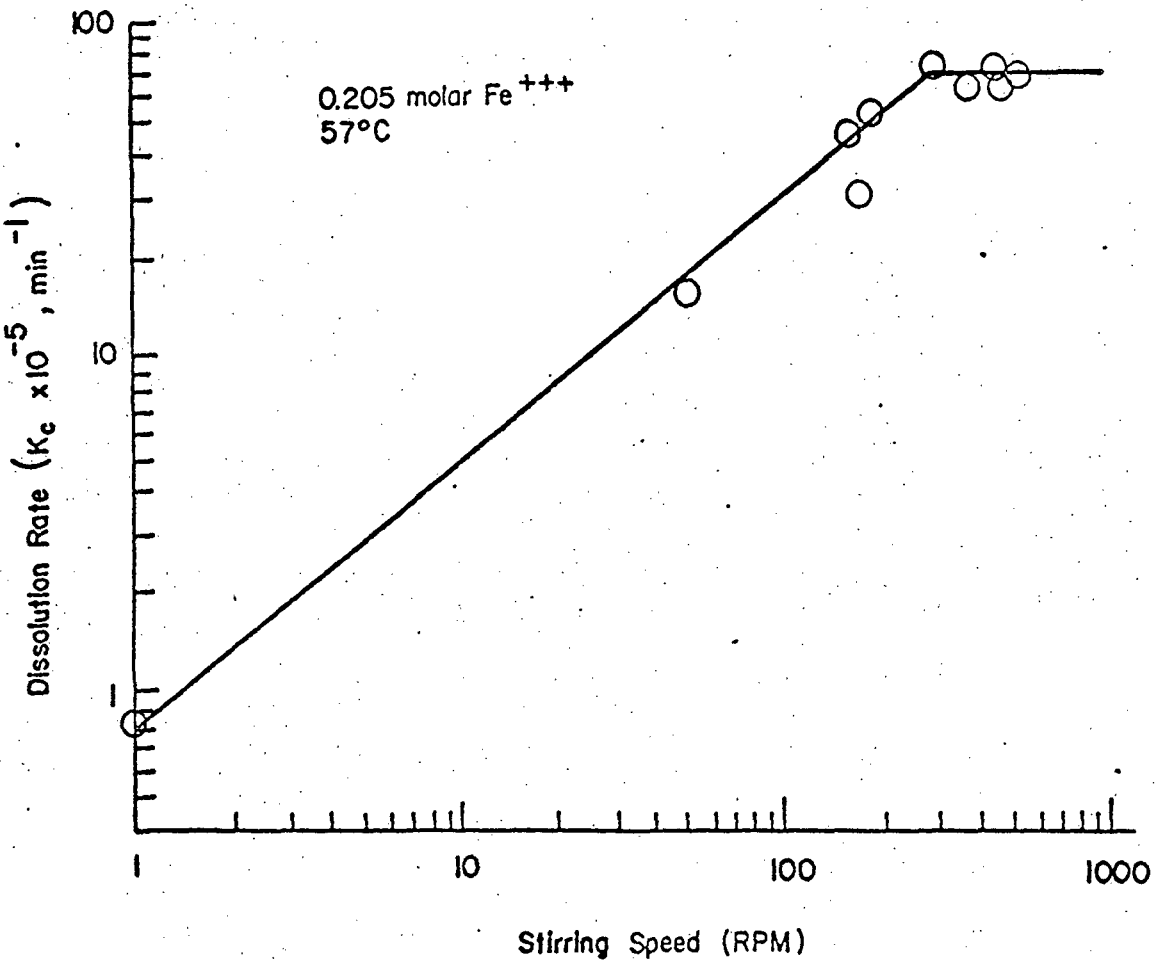

FIGURE 7.--EFFECT OF STIRRING SPEED ON RATE OF DISSOLUTION AT 0.205 MOLAR FERRIC AND 57°C.

Table 2.-- Stoichiometric requirement of Fe^{+++} for sphalerite dissolution reaction

Sample No.	Time (min.)	Dissolved Zn^{++} (g)	Fe^{++} ions formed* (g)	Fe^{++}/Zn^{++}
1	5	0.179	0.420	2.35
2	10	0.328	0.387	1.18
3	15	0.400	0.632	1.58
4	20	0.495	0.755	1.53
5	30	0.710	1.041	1.47
6	40	0.873	1.408	1.61
7	50	1.032	1.907	1.85
8	60	1.186	1.959	1.65
9	80	1.316	2.670	2.02
10	100	1.530	2.687	1.76
11	120	1.587	3.282	2.07
12	140	1.763	3.174	1.80
13	150	1.854	3.327	1.77
14	160	1.802	3.300	1.83
15	170	1.705	3.200	1.88
16	180	1.925	3.550	1.84
	Average---	1.11	2.12	1.91

* Ferrous ions were determined by the method of dichromate titration (Kolthoff, 1957).

where $a \leq 1$. The value of "a" obtained by plotting the logarithm of rate of dissolution against the logarithm of speed of stirring (fig. 7) is 0.75 for liquid diffusion.

Above 300 rpm, the process is independent of the speed of stirring and is no longer controlled by diffusion of a reactant or product through the liquid boundary layer. The rate determining step will then be either chemical reaction at the sulfur-sulfide interface, or diffusion through the sulfur layer, or a combination of these.

Table 3.--Kinetic data of sphalerite dissolution at different speeds

Particle size -100+150 mesh, Fe^{+++} 0.205 molar,

Temperature 57°C, Sample source: St. Joe Minerals Co.

Test No	Stirring speed (rpm)	Kinetic rate (K_c, $min.^{-1}$)	Leaching time (min.)
R-1	460	0.67×10^{-3}	180
R-2	425	0.73×10^{-3}	180
R-3	360	0.56×10^{-3}	180
R-4	155	0.49×10^{-3}	180
R-5	185	0.55×10^{-3}	180
R-6	295	0.75×10^{-3}	180
R-7	360	0.68×10^{-3}	180
R-8	50	0.16×10^{-3}	180
R-9	170	0.31×10^{-3}	180
R-10	0	0.09×10^{-4}	180

In all subsequent experiments the stirring speed was set about 360 rpm so that the liquid diffusion resistance was minimized through the stagnant layer immediately surrounding the particles.

Kinetics--Controlling Step of Reaction

One possible objective of kinetic studies of a dissolution reaction of this type is to determine which step or steps are rate controlling. Some possible steps in the reaction are (1) chemical reaction at the liquid-solid interface or at the sulfur-sulfide interface and (2) the diffusion of products or reactants through the sulfur layer. A typical example for illustrating the reaction steps is shown in figure 8; the curves are given for zinc concentrate leached at 87°C and 360 rpm with ferric ion concentration of 0.25 molar. Two functions, $[1-(1-R)^{1/3}]$ in Equation (6) and $[1 - \frac{2}{3}R-(1-R)^{2/3}]$ in Equation (5), are plotted against the reaction time, t. These two functions relate the fraction reacted, R, as a function of time, t, according to two different models.

In figure 8, it can be seen that neither gives a straight-line relationship throughout the dissolution process. Below about 60 percent completion, the data are linear with respect to the chemical control model, whereas above 60 percent completion, the data are linear with respect to the diffusion control model.

Verification of the possible change in the rate determining step during the leaching process may be obtained by determining how the dissolution of

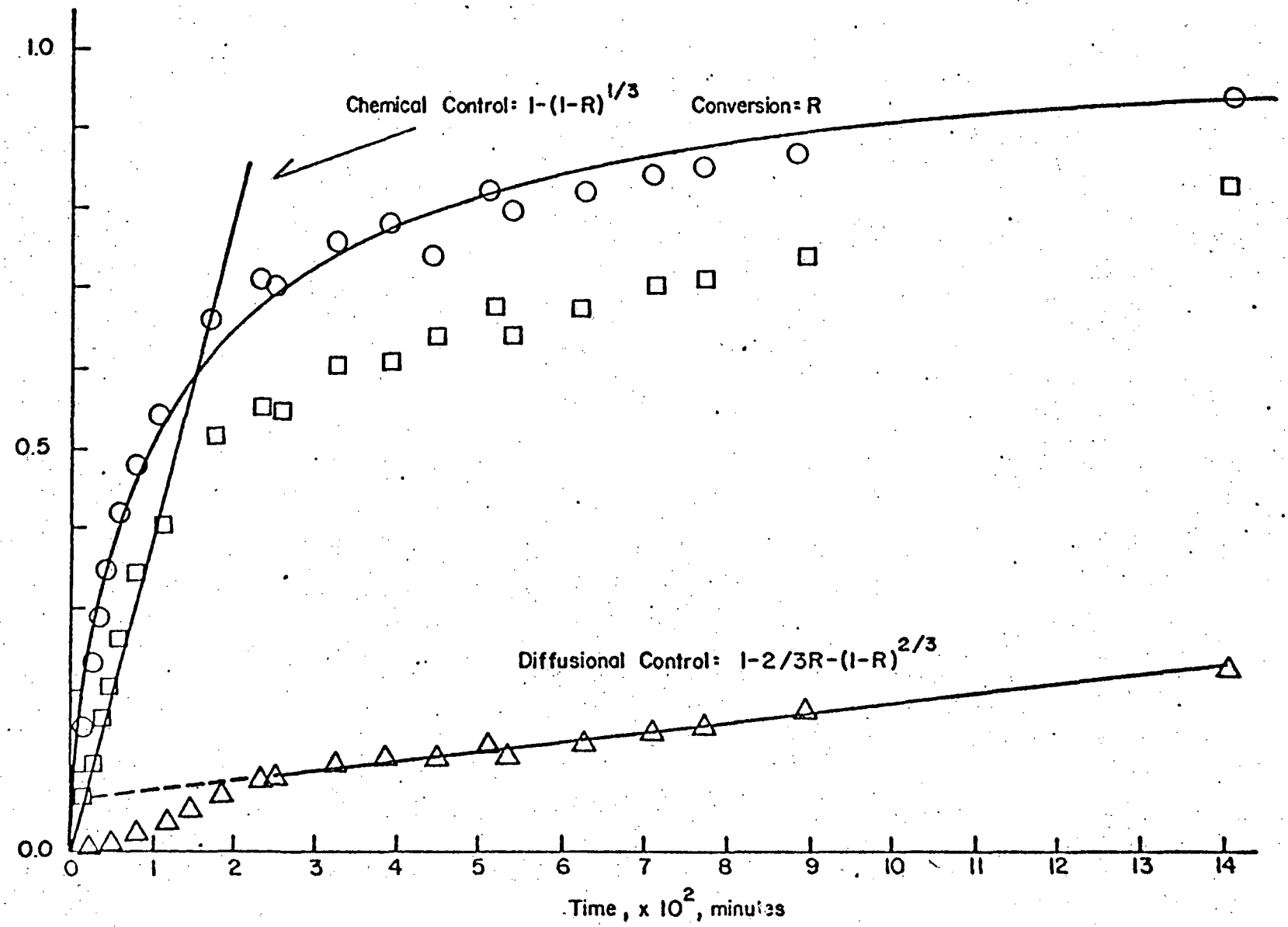

FIGURE 8.--PLOT OF DATA ACCORDING TO CHEMICAL REACTION AND DIFFUSIONAL KINETICS.

concentrates is influenced by particle size. As discussed in previous sections, for the chemical control models, time and fraction reacted are related according to Equation (6).

$$1 - (1-R)^{1/3} = \frac{bk_{cc}C_{fl}M}{P_z} \times \frac{1}{r_o} \times t \qquad (6)$$

Rearrangement of Equation (6) gives in logarithmic form:

$$\log t = \text{Log } A_1 + \log r_o$$

where

$$A_1 = \frac{1 - (1-R)^{1/3} P_z}{bK_{cc}C_{fl}M}$$

or $\log t \backsim \log r_o$

A plot of log r_o vs log t will give a slope of one. Similarly, for the diffusion control model, the reaction rate is given by Equation (5):

$$1 - \frac{2}{3}R - (1-R)^{2/3} = \frac{2bMD_eC_{fs}}{P_z} \times \frac{1}{r_o^2} \times t$$

Rearranging and taking logs gives:

$$\log t = \log A_2 + 2 \log r_o$$

$$\text{or} \quad \log t \backsim 2 \log r_o$$

where

$$A_2 = \frac{Pz}{2bMD_eC_{fs}} \times \frac{1 - \frac{2}{3}R - (1-R)^{2/3}}{1}$$

A slope of log r_o vs log t will give a slope of two.

A series of experiments was run for different particles sizes, (-28 + 35 mesh, -35 + 48 mesh, -48 + 65 mesh, -65 + 100 mesh, -100 + 150 mesh, -150 + 200 mesh) under the same leaching condition. The time needed to achieve the same fractional conversion for each particle size was plotted against particle size, log r_o. Figure 9 and table 4 show the results of these experiments. The five lines each represent a constant value of R, the fraction reacted for a series of particle sizes. The slope of the line R = 20% is about one, and the slope of the line for R = 95% is slightly greater than two.

The slope changes continuously from about one to about two. This may be interpreted that Reaction (1) is controlled by a combination of the two models.

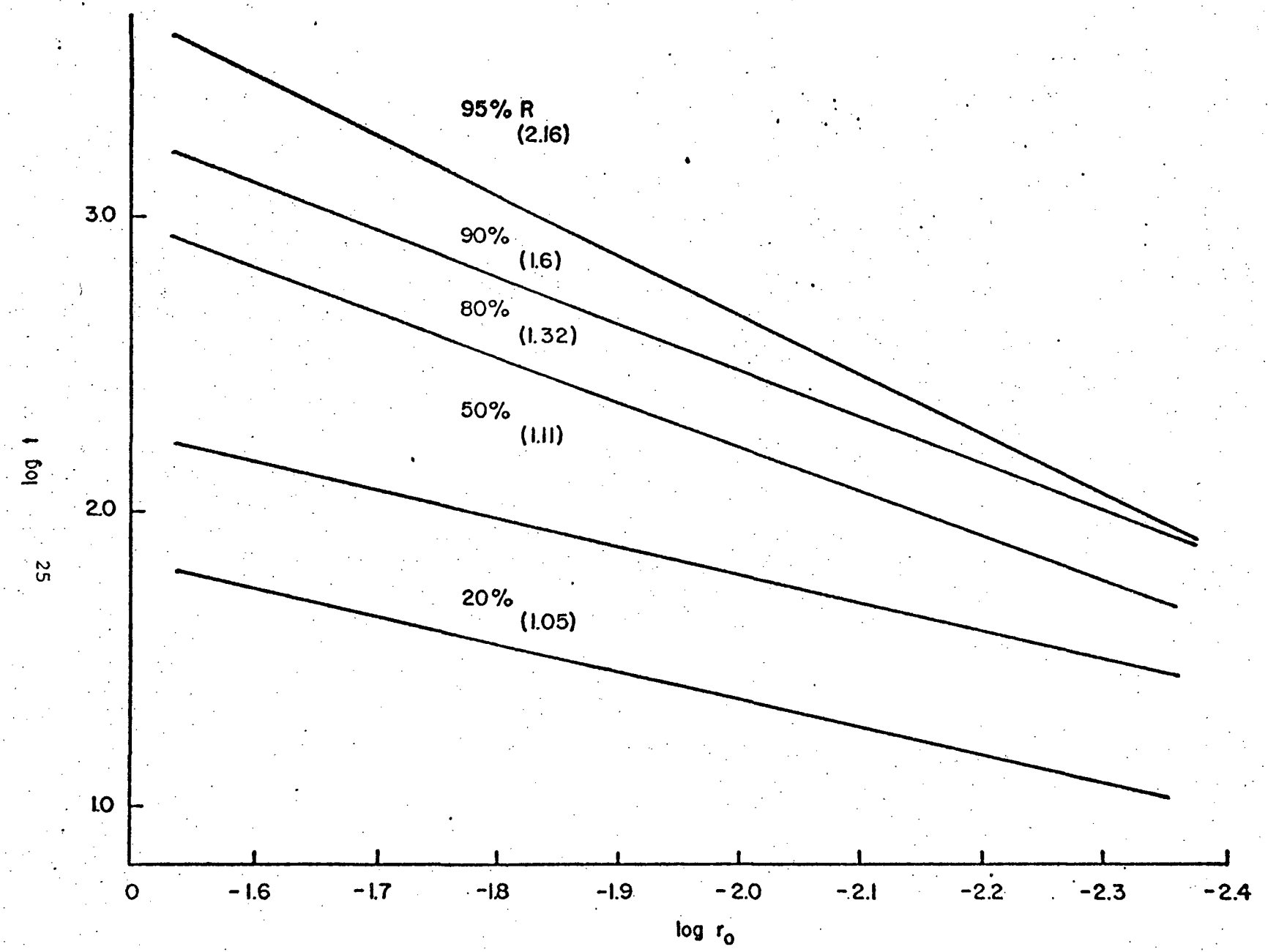

FIGURE 9.--PLOT OF LOG TIME VS. LOG MINERAL PARTICLE'S RADIUS (BY REGRESSION).

Table 4.--Regression Analysis of log radius of mineral particle and log time in leaching

Run No.	Particle Size (mesh)	Radius (cm)	Log Time Required for Different Fraction R% 20%	50%	80%	90%	95%
R-51	-38+35	0.02515	1.81	2.40	3.06	3.51	4.23
R-52	-35+48	0.01780	1.70	2.30	2.81	2.97	3.06
R-53	-48+65	0.01255	1.56	2.06	2.52	2.74	2.76
R-54	-65+100	0.00890	1.30	1.93	2.36	2.53	2.55
R-11	-100+150	0.00625	1.30	1.78	2.32	2.48	2.55
R-55	-150+200	0.00445	1.00	1.57	2.00	2.18	2.30
Regression coefficient-------			1.05	1.11	1.32	1.60	2.16
Constant term----------			3.52	4.19	5.12	5.86	7.17
Correlation coefficient------			0.98	0.99	0.98	0.96	0.88

It is desirable to combine the above two steps, chemical and diffusion, into one mixed-control equation, and then study the variation of each resistance to Reaction (1) of this mixed-model equation with the particular variable of interest. Equation (7) is a mixed-model equation for spherical particles:

$$\frac{MbK_{cc}D_eC_{fs}}{P_z\, r_o^2} \cdot t = \frac{K_{cc}}{2}\left[1 - \tfrac{2}{3}R - (1-R)^{2/3}\right] + \frac{D_r}{r_o}\left[1 - (1-R)^{1/3}\right] \qquad (7)$$

Here, rearranging Equation (7) by multiplying each term by r_o/D_e, the following relationship is obtained

$$\frac{MbK_{cc}C_{fs}}{P_z r_o} \cdot t = \left[(1 - (1-R)^{1/3}\right] + \frac{K_{cc}}{2}\frac{r_o}{D_e}\left[1 - \tfrac{2}{3}R - (1-R)^{2/3}\right]$$

or

$$K_r t = \left[1 - (1-R)^{1/3}\right] + B\left[1 - \tfrac{2}{3}R - (1-R)^{2/3}\right] \qquad (9)$$

The reaction rate in this case is controlled in part by the rate of reaction at the interface and in part by diffusion. The total resistance to the overall reaction is the sum of the two factors on the right side of Equation (9), whose terms may be identified respectively as the interface or chemical reaction resistance and the sulfur or diffusion resistance.

Figure 10(a) and 10(b) appear to be repetitions of figure 8. Figure 10(a) illustrates typical data plotted against the diffusion control term of Equation (9). The data give a straight line only after about R = 0.4. These same data plotted against the chemical control term of Equation (9) in figure 10(b)

indicate that a linear relationship is obtained up to R = 0.4. When these data are plotted against the right side of Equation (9), a straight line is obtained which passes through the origin. The transition points between the chemical control and the diffusion control are at the point of 40% conversion, R, as shown in figure 10(a) and (b). The transition points from all experimental data are between 25% and 60%. Equation (9) is applied to the case of instantaneous ferric ions concentration $C_{fs} = C_o - C_t$. C_o is the original concentration of ferric ions and C_t is the amount of ferric ion per liter consumed at time, t. $C_o - C_t$ is the ferric ion concentration remaining at time t. If the experimental conditions permit the ferric ion concentration to remain nearly constant such that $C_o - C_t = C_o$, then C_t may be neglected and thus $C_{fs} = C_o$.

Determination of Chemical Rate Constant, K_{cc}, and Diffusion Coefficient, D_e

When the chemical reaction at the sulfide-sulfur interface is the rate determining step, the data will plot linearly when the quantity $1 - (1-R)^{1/3}$ [Equation (6)] is plotted against the reaction time, t. From Equation (6) is

$$1 - (1-R)^{1/3} = K_c t$$

where

$$Kc = \frac{MbK_{cc}C_{fc}}{P_z r_o} \qquad (6)$$

The slope of this line is K_c from which the chemical rate constant K_{cc} can be obtained by calculation from the other constants P_z, r_o, C_{fc}, and b.

Similarly, when diffusion through the product layer is the rate controlling step the kinetics will be linear according the Equation (5) when the quantity $1 - \frac{2}{3}R - (1-R)^{2/3}$ is plotted against the reaction time t.

$$1 - \tfrac{2}{3}R - (1-R)^{2/3} = K_p t \qquad (5)$$

where $K_p = \dfrac{2bMD_eC_{fs}}{P_z r_o^2}$

Rate Dependence on Ferric and Ferrous Ion Concentration

Experiments were done to establish the dependence of the rate of dissolution on the ferric ion concentration. The experiments were run at 87°C and 360 rpm with the ferric iron concentration varied from 0.0125 molar to 0.8 molar. Table 5 gives the kinetic data obtained from 16 leaching experiments using zinc concentrates and nine using polished sphalerite crystals. These data indicate that, for concentrations between 0.0125-0.1 molar ferric ion, the dissolution rate is proportional to the concentration of ferric ion but is insensitive to ferric ion concentration above 0.1 molar (fig. 11). The slope of the straight

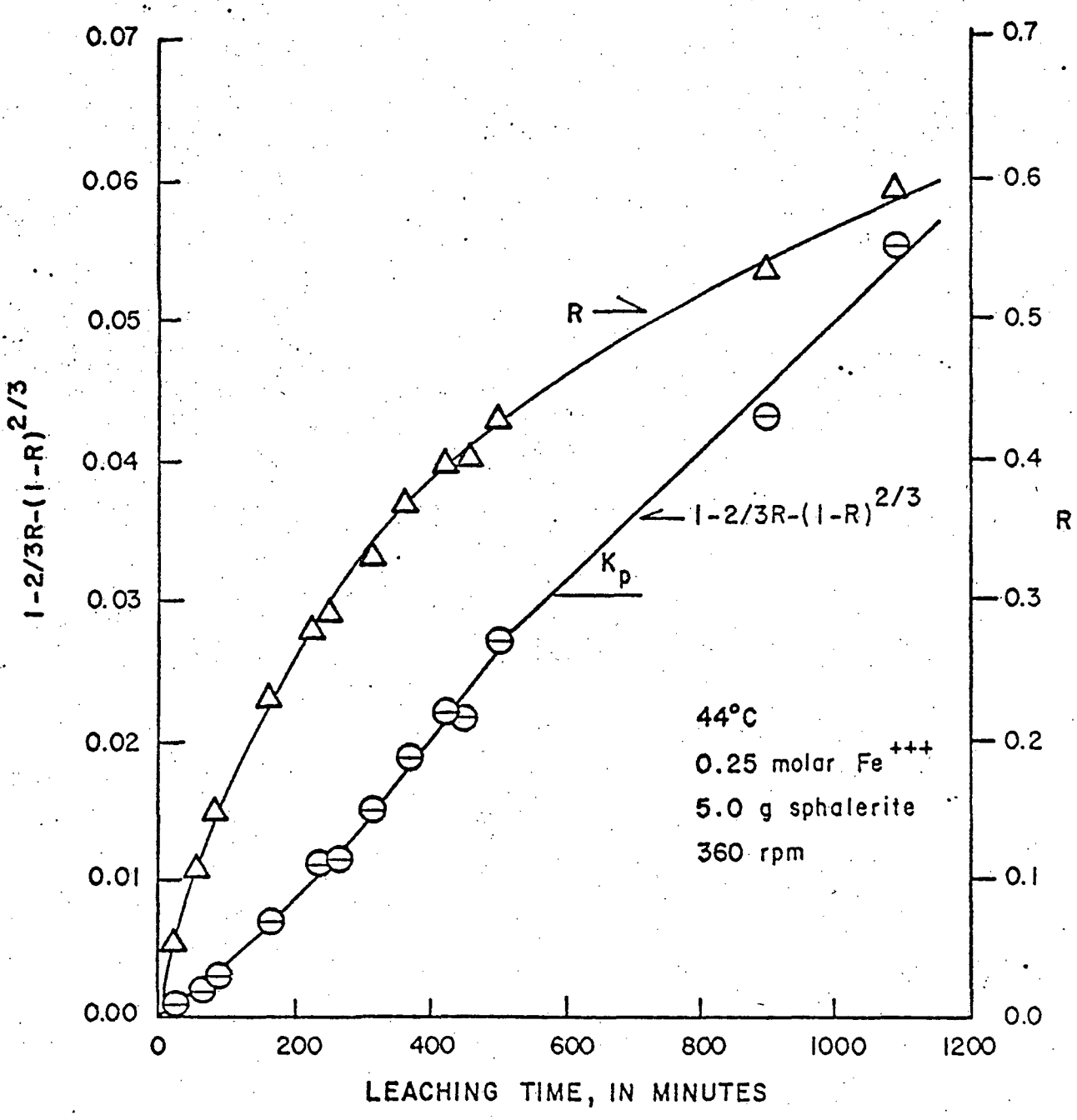

FIGURE 10(A).--A TYPICAL PLOT OF REACTION DATA ACCORDING TO DIFFUSIONAL CONTROL MODEL.

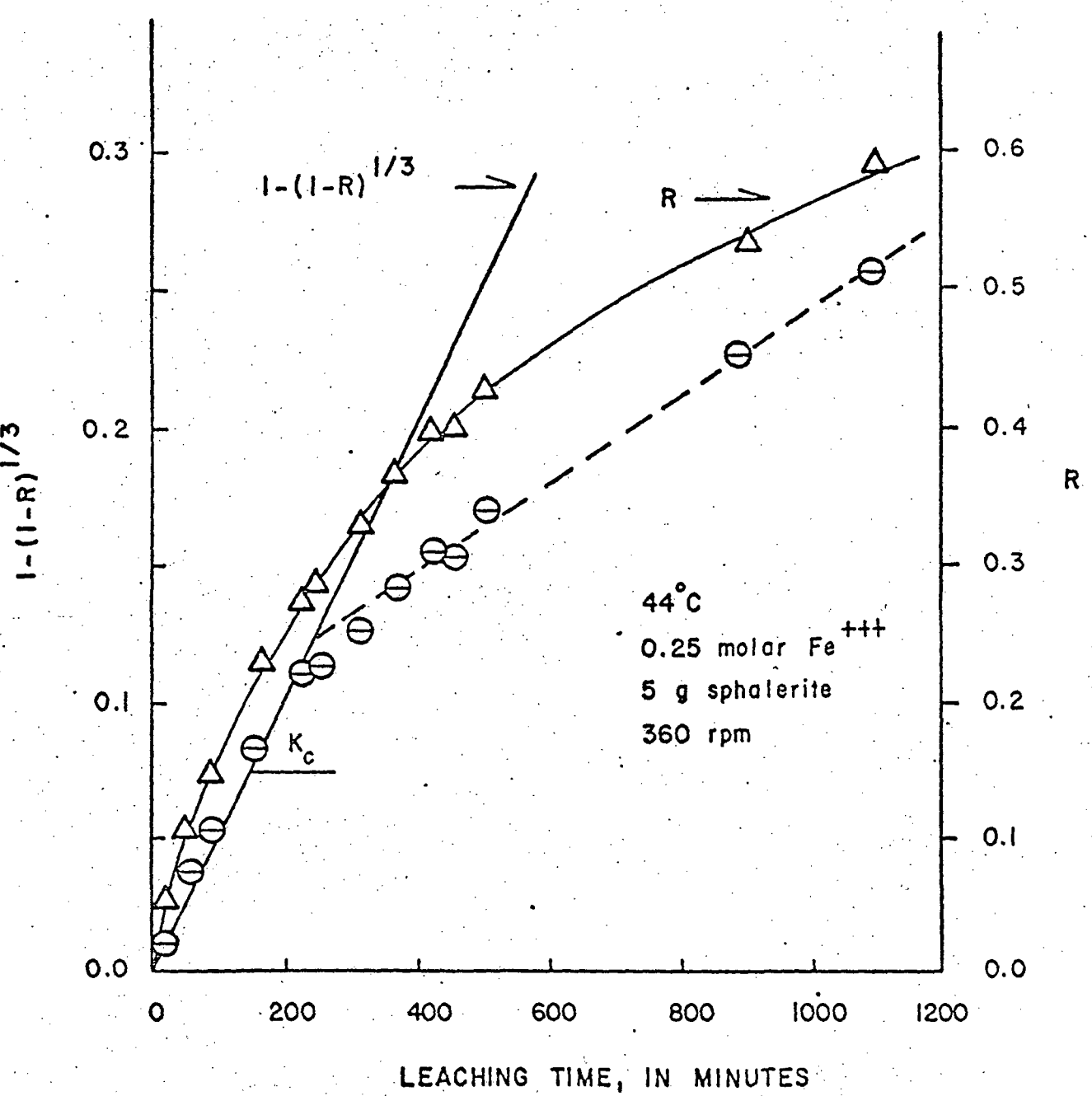

FIGURE 10(B).--CHEMICAL CONTROL MODEL.

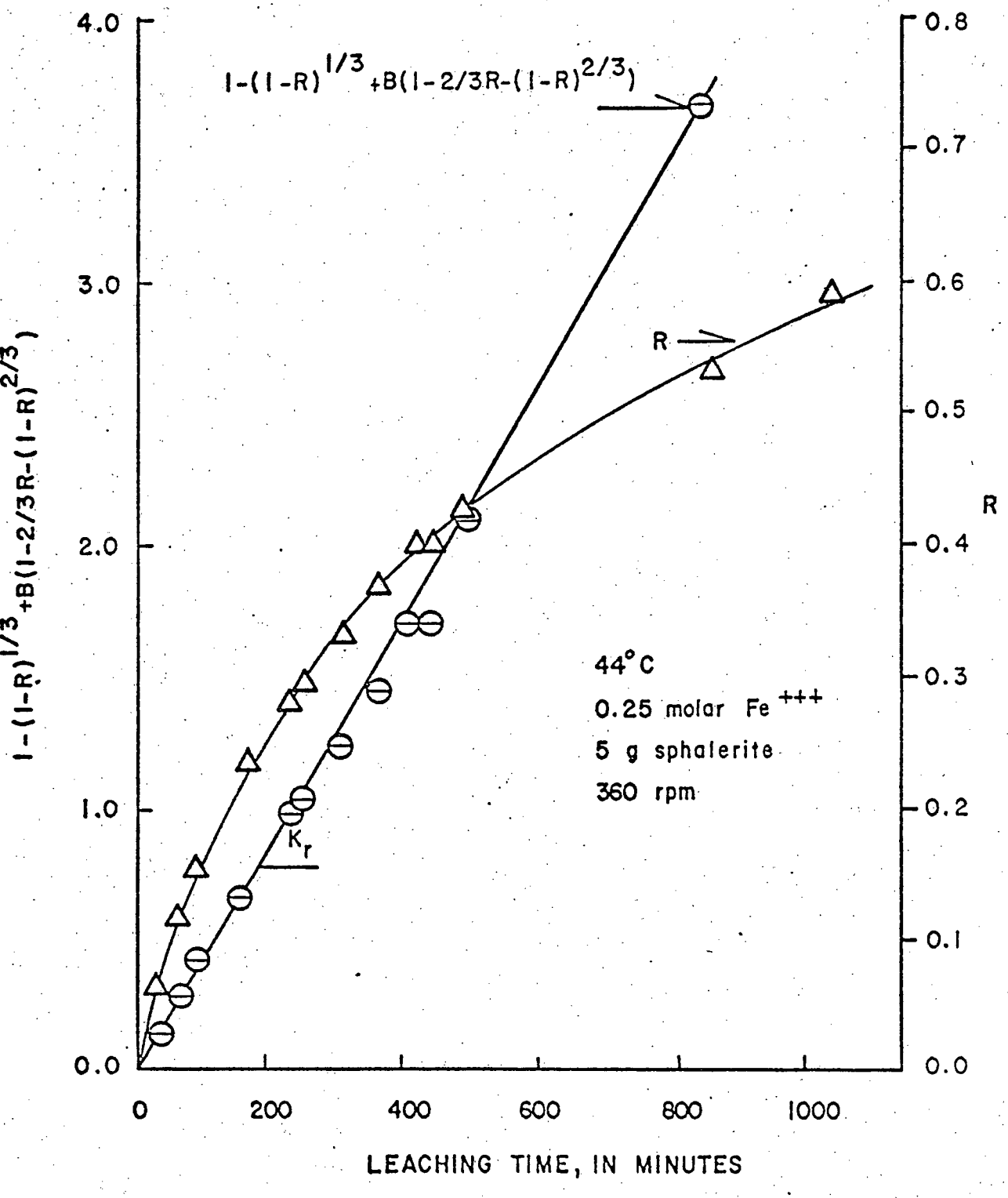

FIGURE 10(c).--MIXED CONTROL MODEL.

line below 0.1 molar Fe^{+++} ion (fig. 11) is 1.1 which indicates a first-order reaction. The first-order dependence of rate of leaching on ferric ions was also noted by Dutrizac and others (1969) in a study of synthetic chalcopyrite in acidic ferric sulfate solutions while the ferric ion concentration was below 0.01 molar. Lowe (1970) reported that the reaction order was also one in the dissolution of chalcocite in ferric sulfate solution (0.007-0.3 molar).

For ferric ion concentrations below 0.1 molar a chemisorption process may be taking place. Chemisorption involves two steps: adsorption and subsequent electron transfer between the adsorbed ion and the solid particle. An electron transfer reaction is essentially the same as the surface reaction. The ferric ion is reduced to ferrous ion according to the reaction, $2Fe^{+++} + 2e \rightarrow 2Fe^{++}$, and the sulfur in ZnS is oxidized to the elemental state according to the reaction, $ZnS \rightarrow Zn^{++} + S^{\circ} + 2e^{-}$.

The rate reaction is a function of the ferric ion concentration and the fraction of active sites covered. The data plotted below 0.1 molar of ferric ion concentration in figure 11 were initial kinetic data obtained during the early stages of leaching, and may be proposed as a chemisorption process. The kinetics below 0.1 molar of ferric ion concentration may be interpreted as liquid diffusion through the stagnant layer immediately around the specimens (Wadsworth, 1972(b)). Though the stirring speed, 360 rpm, is high enough to eliminate diffusional control through the stagnant layer around the sample, it is not expected to eliminate diffusion control through the sulfur layer. However, the activation energy may determine which mechanism may dominate the process.

The activation energy of chemisorption below 0.1 molar Fe^{+++} ion concentration is 15.4 Kcal per mole with a first-order reaction (fig. 12). Taylor (1931) reported that the activation energy of water adsorbed at a bauxite surface was about 21 Kcal per mole, which indicates the adsorption processes may involve large energies of activation and high heats of adsorption with the result that the adsorption process itself is the slow step (Wadsworth and Malouf, 1972b). Surana and Warren (1969) proposed a common mechanism of leaching involving anion adsorption and activation of the mineral surfaces for geothite and hematite. The activation energy quoted for leaching in sulfuric acid was 19.9 Kcal/mole and in hydrochloric acid 22.5 Kcal/mole. Both are the first-order reactions.

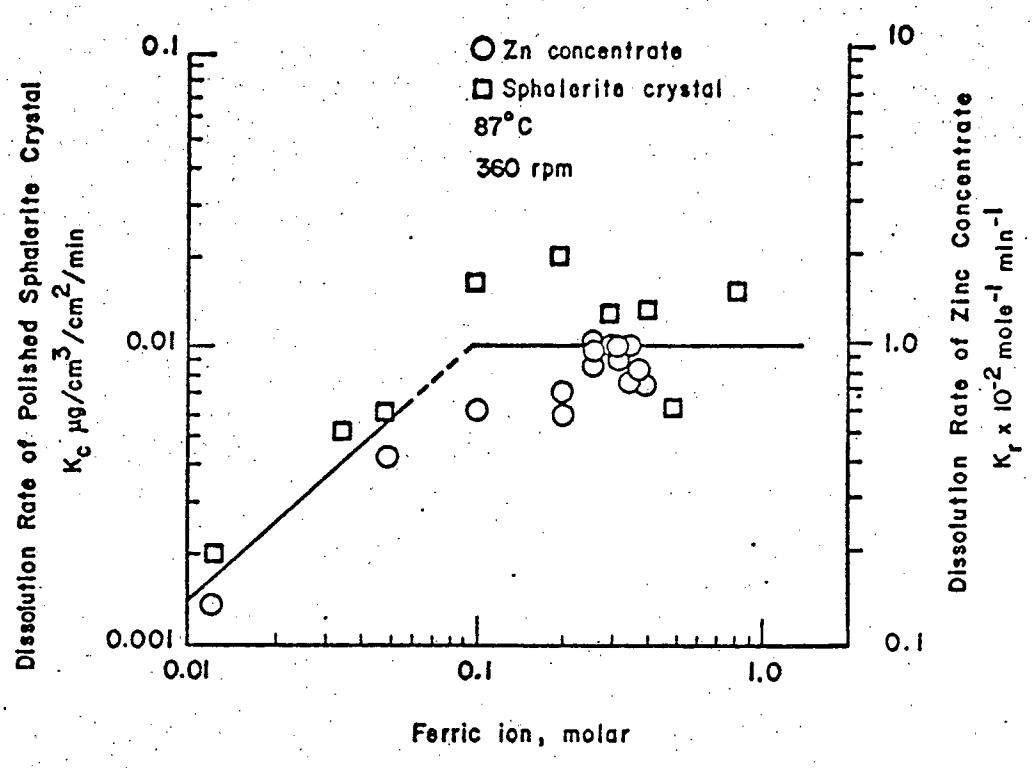

FIGURE 11.--DISSOLUTION RATE AS A FUNCTION OF FERRIC ION CONCENTRATION.

When the concentration of ferric ion is above about 0.1 molar, a mixed-kinetics is proposed. The slope of horizontal line in figure 11 is zero, which indicates a zero-order reaction and means that the rate of reaction is independent of ferric iron concentration. Lowe (1970) also observed a zero-order reaction in the dissolution of chalcopyrite in ferric sulfate solution.

As previously discussed, the rate-controlling step may involve the outward diffusion of products, Zn^{++} or Fe^{++}. To test whether the outward diffusion of ferrious ion controlled the reaction rate, experiments were run on the polished sphalerite crystal with constant ferric ion concentration 0.25 molar and containing $FeCl_2$ concentrations of up to 60%. In concentrations above 60%, it is difficult to determine the zinc ion concentration, because the amount of zinc in solution is too low to be measured by atomic absorption. The experimental results are shown in figure 13 and listed in table 6. The leaching rate evidently decreases with an increase of ferrous iron in the bulk solution. The deviation from linearity in fig. 13 indicates that the activity coefficient of Fe^{++} ion increases as the Fe^{++} ion concentration increases.

The rates of dissolution were controlled by the gradient of Fe^{++} concentration across the sulfur layer as expressed in the following equation

$$\text{Rate} = \frac{D_e}{\delta} A \left[(a_{Fe^{++}})\ \text{saturated} - (a_{Fe^{++}})\text{bulk}\right] \qquad (10)$$

where D_e : diffusion coefficient, cm^2/min

δ : sulfur layer thickners, cm

A : surface area (constant), cm^2

$[a_{Fe^{++}}]$ saturated: concentration of Fe^{++} at the sphalerite/solution surface is assumed to be saturated.

$[a_{Fe^{++}}]$ bulk: concentration of Fe^{++} in the bulk solution.

Because the concentration of ferrous iron in the bulk solution ranges widely, the gradient of Fe^{++} concentration across the sulfur layer, $[(a_{Fe^{++}})\ \text{saturated} - (a_{Fe^{++}})_{\text{bulk}}]$, also ranges widely and so does the dissolution rate.

However, in most cases, during the later stages of leaching, the concentration of ferric ions is depleted if no make-up concentration of ferric ions is supplied. Then, a point will be reached where the inward diffusion of ferric ions is slower than the outward diffusion of ferrous ion. In this case, the inward diffusion of ferric ion becomes rate controlling. Such a point of view was also taken by Dutrizac and others (1969) in their report of dissolution of synthetic chalcopyrite in aqueous acidic ferric sulfate solutions.

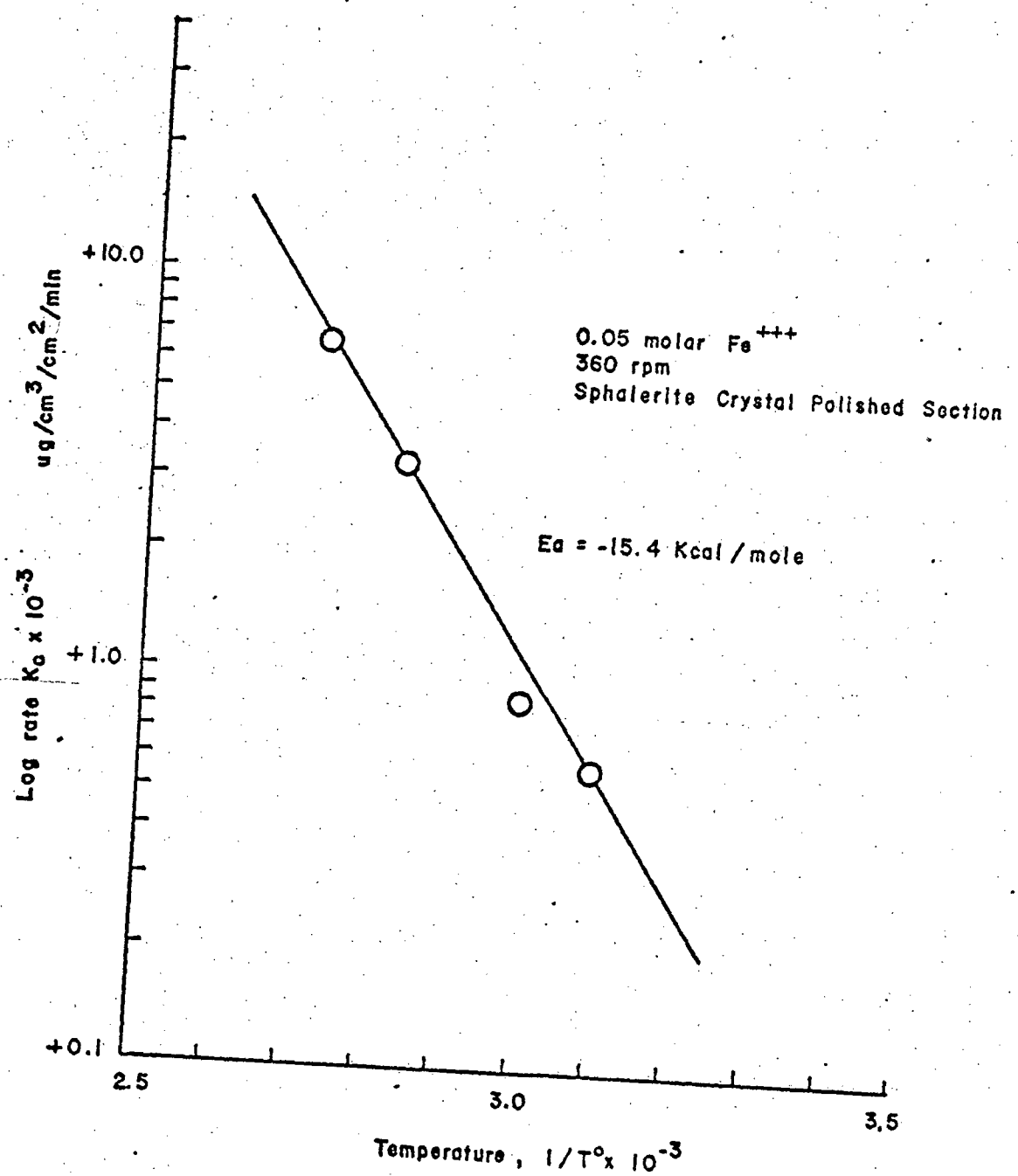

FIGURE 12.--ARRHENIUS PLOT OF LOG K_c VERSUS $1/T°K$.

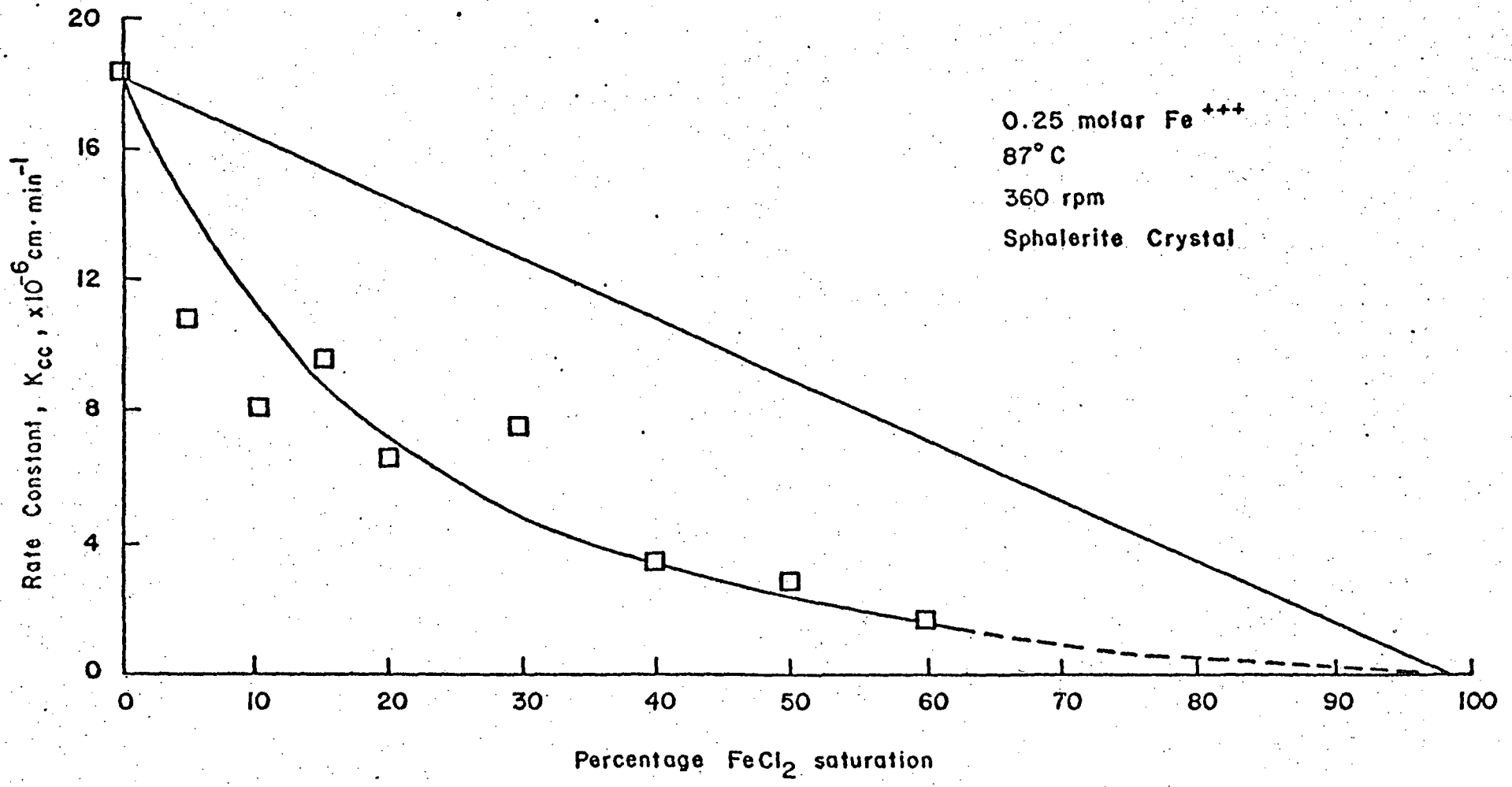

FIGURE 13.—EFFECT OF INITIAL $FeCl_2$ CONCENTRATION ON THE RATE OF DISSOLUTION.

Table 5.--Effect of Fe^{+++} ion concentration on dissolution kinetic at 87°C and 360 rpm

Test No.	Fe^{+++} Concentration (molar)	Rate Constant (K_{cc} cm/min) $\times 10^{-3}$	Diffusion Coefficient (D_e, cm^2/min) $\times 10^{-5}$	Dissolution K_r $mole^{-1} \cdot min^{-1}$ $\times 10^{-2}$	Rate min^{-1} $\times 10^{-2}$
Zinc Concentrate (-100 + 150 mesh)					
R-11	0.250	10.2	1.42	3.8	0.96
R-12	0.103	10.6	0.90	6.0	0.62
R-13	0.051	12.0	0.90	8.0	0.41
R-14	0.013	10.0	0.90	10.0	0.13
R-15	0.328	8.0	0.60	3.0	0.98
R-16	0.411	5.0	0.35	2.0	0.80
R-17	0.250	8.0	1.42	4.0	1.00
R-18	0.337	7.0	0.50	2.8	0.94
R-19	0.250	9.0	1.40	3.6	0.90
R-20	0.205	11.0	1.40	2.8	0.57
R-21	0.205	10.0	1.40	3.5	0.72
R-22	0.328	7.0	0.60	3.0	0.98
R-23	0.328	6.0	0.50	3.0	0.98
R-24	0.367	5.0	0.35	2.2	0.80
R-25	0.367	6.0	0.35	2.2	0.81
R-26	0.287	10.6	0.30	3.2	0.92

Test No.	Fe^{+++} Concentrate (molar)	Kc	Rate $g/cm^3/cm^2/min$
Sphalerite Crystal			
R-73	0.200		0.020
R-74	0.100		0.016
R-75	0.050		0.006
R-76	0.250		0.005
R-77	0.013		0.002
R-78	0.290		0.013
R-79	0.400		0.013
R-80	0.500		0.006
R-81	0.800		0.015

Table 6.--Dissolution rate as a function of Fe(II) concentration at 87°C and 360 rpm (sphalerite crystal)

Test No.	Surface Area (cm^2)	F^{+++} Concentration (molar)	Fe^{++} Saturation (%)	Rate Constant K_{cc} (cm/min^{-1})	Leaching Time (min.)
R-61	0.9881	0.25	5	10.8×10^{-6}	630
R-62	0.9881	0.25	10	8.2×10^{-6}	360
R-63	0.9881	0.25	15	9.8×10^{-6}	250
R-64	0.9881	0.25	20	6.3×10^{-6}	840
R-65	0.9881	0.25	30	7.8×10^{-6}	645
R-66	0.9881	0.25	40	3.6×10^{-6}	600
R-67	0.9881	0.25	50	3.3×10^{-6}	665
R-68	0.9881	0.25	60	1.7×10^{-6}	735
R-57	1.1050	0.25	0	18.8×10^{-6}	760

Effect of Temperature

Samples of the sphalerite concentrate in the -100 + 150 mesh range were leached in temperatures ranging from 44° to 90°C to determine the effect of temperature on the rate of Reaction (1). See figure 14 and table 7. The data are plotted in terms of the function $[(1 - (1\ R)^{1/3} + B\ (1 - \frac{2}{3}R - (1-R)^{2/3}]/(C_o - C_t)$ against time, t. This function was found to fit the data best for the overall reaction process. The slopes, $K_r = MbK_{cc}/P_z r_o$ (Equation 9) of the lines are steeper as the temperature increases which would be expected since the chemical reaction rate constant, K_{cc}, increases exponentially with temperature.

The activation energy, E_a, for the reaction can be obtained from the exponential variation of this constant K_{cc} with temperature, t. Taking the log of both sides of the Arrhenius equation, $K_{cc} = Fe^{-E_a/RT}$, gives:

$$\log K_{cc} = \log F - \frac{E_a}{2.303\ RT} \qquad (11)$$

F : Frequency factor

by plotting $\log K_{cc}$ vs 1/T, a straight line is obtained as shown in figure 15. Least squares analysis of the data used to construct figure 15 gives

$$\log K_{cc} = -4.78 + 2.45 \times \frac{10^3}{T} \qquad (12)$$

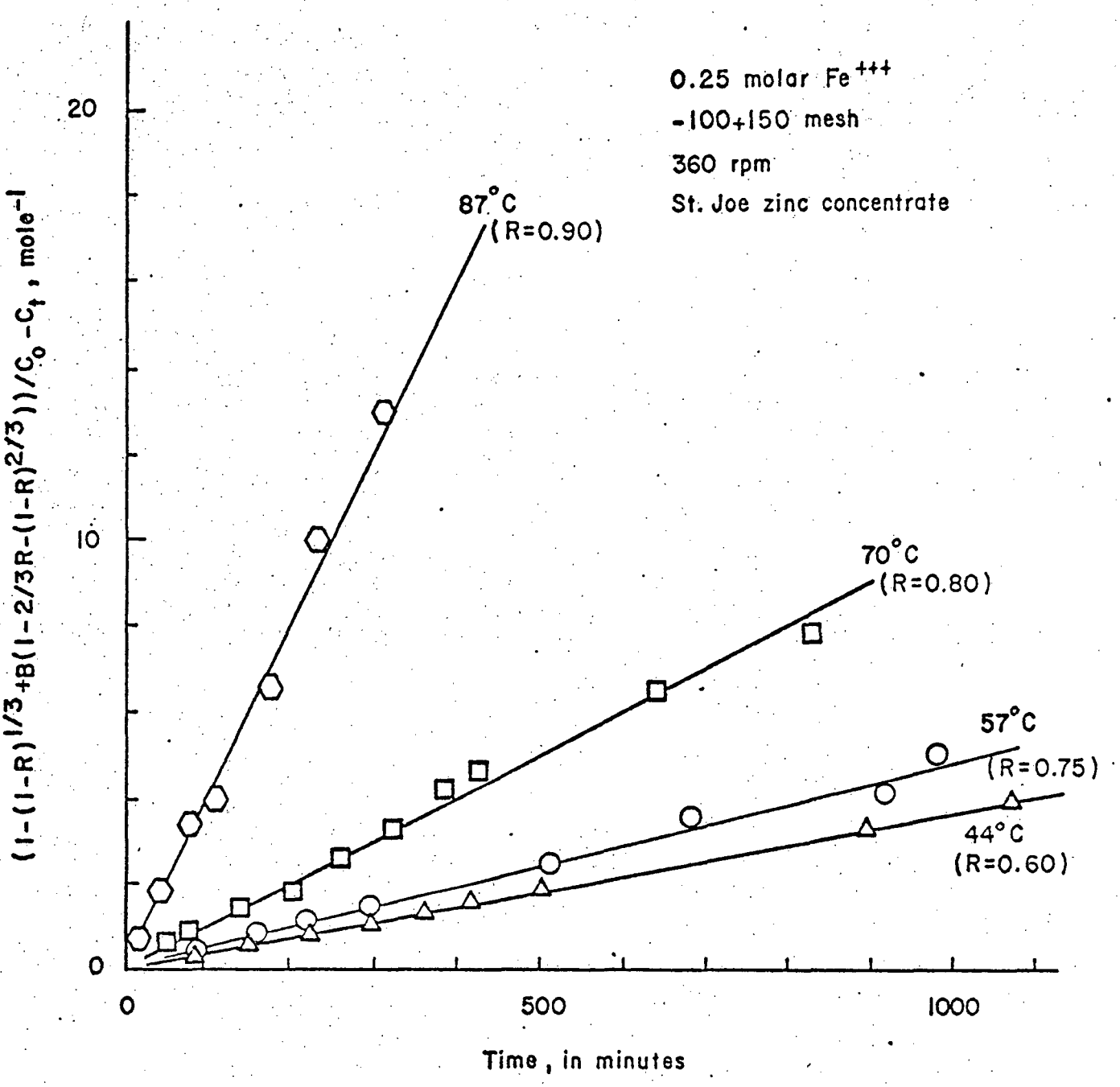

FIGURE 14.--DEPENDENCE OF REACTION RATE ON TEMPERATURE.

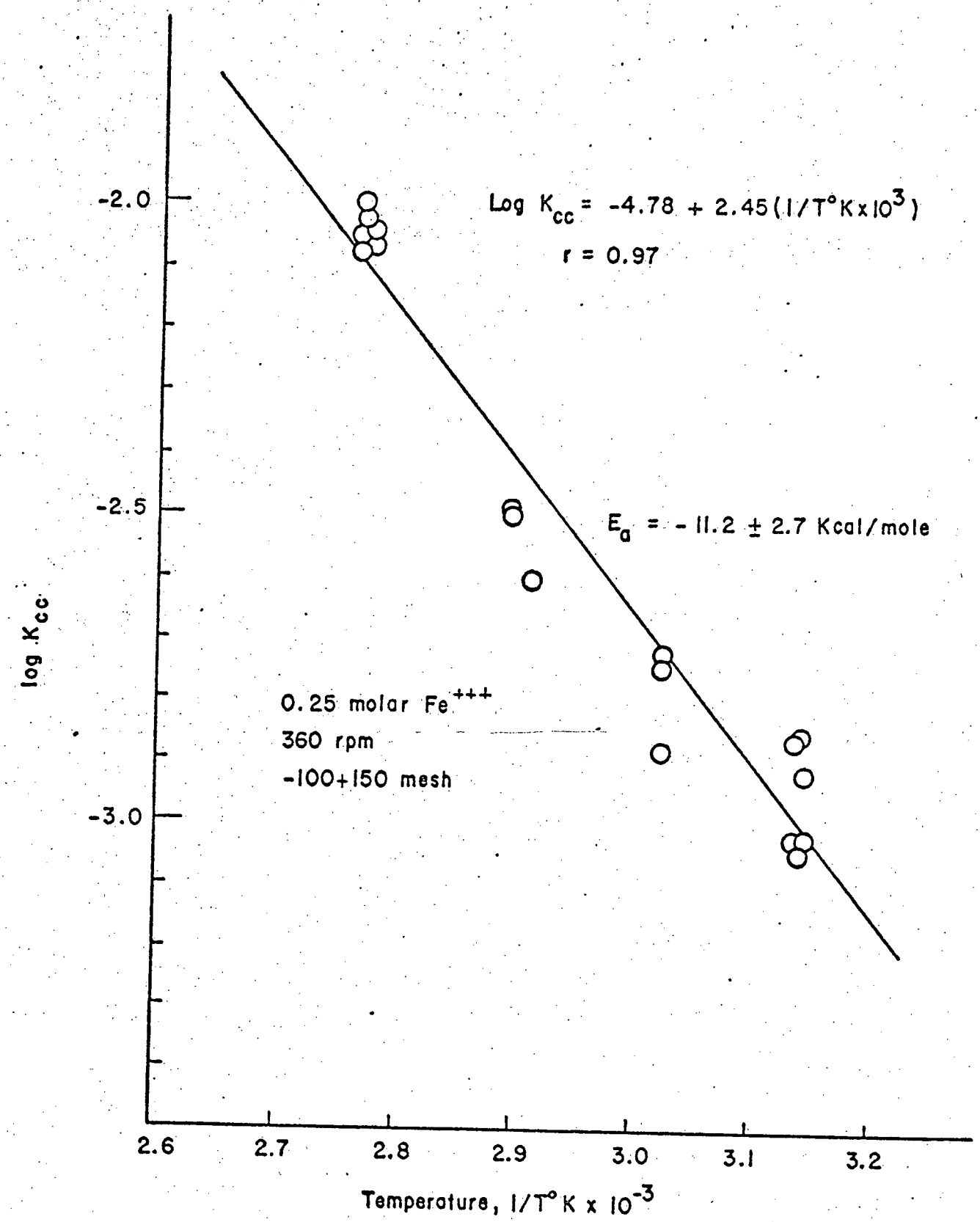

FIGURE 15.--ARRHENIUS PLOT OF LOG K_{CC} VERSUS 1/T°K.

From this the value for the activation energy $E_a = -11.2 \pm 2.7$ Kcal is obtained from the regression coefficient 2.45 which is equal to $\frac{-E_a}{2.303 \times R \times R10^{-3}}$. The 95% confidence interval for the mean has a value of $\pm$ 2.7 Kcal/mole. According to Habashi (1970), the activation energy of a diffusion controlled process through a liquid boundary is approximately 1 to 3 Kcal/mole, whereas for a chemically controlled process it is usually greater than 10 Kcal/mole. However, in a mixed-kinetic process which involves pore diffusion, the activation energy is much greater than that for liquid boundary diffusion, and can be comparable to that for chemical reaction controlled process. Pohlman and Olson (1974) reported a mixed-kinetics model for the acid leaching of chrysocolla. They determined an activation energy of 8 Kcal per mole for the overall reaction process which is consistent with the experimental activation energy reported here, that is 11.2 $\pm$ 2.7 Kcal/mole.

Effect Of Initial Particle Size

The effect of surface area on the rate of leaching was studied by determining the rate of dissolution of six fractions of concentrate sizes, -28 + 35 mesh, -35 + 48 mesh, -48 + 65 mesh, -65 + 100 mesh, -100 + 150 mesh, and -150 + 200 mesh. The rate of dissolution, as expected, was found to increase with decreasing particle size or with increasing surface area (fig. 16). As the particle size decreases, the rate of dissolution increases for a given period of time. From table 8 the constant B in Equation (9) is an indirect function of particle size if other factors are constant. The rate constant, K_{cc}, is independent of particle size, but the reaction rate, K_r, is particle size dependent.

Equation (9), $K_r t = 1 - (1-R)^{1/3} + B\,[1 - \frac{2}{3}R - (1-R)^{2/3}]$, can be rewritten rewritten as $X + Y = K_r t$, where K_r is reaction rate and X represents the percent contribution to the rate due to reaction at the sulfur-sulfide interface, $1 - (1-R)^{1/3} \;/\; 1 - (1-R)^{1/3} + B\,[1 - \frac{2}{3}R - (1-R)^{2/3}]$, and Y the diffusion controlled portion, $B\,[1 - \frac{2}{3}R - (1-R)^{2/3}] \;/\; 1 - (1-R)^{1/3} + B\,[1 - \frac{2}{3}R\,(1-R)^{2/3}]$. By comparing the relative magnitude of the contribution of the surface reaction, X, and of the diffusion, Y, to the total kinetics it can be determined which mechanism is dominant as the particle size is changed. A comparison of this type has been made in figure 17 for two particle sizes. Data were plotted, X, the chemical reaction percentage in total kinetics against the fraction reacted,

Table 7.--Dependence of rate constant, K_{cc}, and effective diffusion coefficient, D_e, on temperature

Test No.	Fe^{+++} Concentration (molar)	Temperature (C^o)	Rate Constant (K_{cc}, cm/min.)	Diffusion Coefficient (D_e, cm /min.)	Leaching Time (min.)
Sample from St. Joe Minerals (particle size -100 + 150 mesh)					
R-27	0.21	87	12×10^{-3}	10×10^{-6}	120
R-28	0.21	44	1.1×10^{-3}	-	120
R-29	0.21	44	1.1×10^{-3}	-	150
R-30	0.21	44	1.1×10^{-3}	-	150
R-31	0.21	57	2.1×10^{-3}	-	150
R-32	0.21	57	1.5×10^{-3}	-	150
R-33	0.21	72	3.6×10^{-3}	-	190
R-34	0.21	87	11×10^{-3}	-	360
R-35	0.25	44	1.1×10^{-3}	0.57×10^{-6}	180
R-36	0.25	57	1.5×10^{-3}	1.6×10^{-6}	180
R-37	0.25	70	2.8×10^{-3}	1.8×10^{-6}	180
R-38	0.25	87	10×10^{-3}	6.8×10^{-6}	1405
R-1	0.21	57	1.7×10^{-3}	-	180
R-2	0.21	57	1.8×10^{-3}	-	180
R-3	0.21	57	1.4×10^{-3}	-	180
R-11	0.25	87	10.2×10^{-3}	14×10^{-6}	535
R-20	0.25	87	10.1×10^{-3}	-	120
R-21	0.25	87	10.0×10^{-3}	8.1×10^{-6}	120
Sample from U.V. Industries, Inc. (particle size -100 + 150 mesh)					
R-39	0.21	87	16×10^{-3}	11×10^{-6}	180
R-40	0.21	72	6.8×10^{-3}	-	120
R-41	0.21	44	1.8×10^{-3}	-	120
R-42	0.21	57	2.4×10^{-3}	-	140
Sample from ASARCO (particle size -100 + 150 mesh)					
R-43	0.21	87	5.5×10^{-3}	-	150
R-44	0.21	87	5.5×10^{-3}	-	150
R-45	0.21	57	1.8×10^{-3}	-	150
R-46	0.21	87	7.0×10^{-3}	-	160
R-47	0.21	72	3.5×10^{-3}	-	150
R-48	0.21	79	6.9×10^{-3}	-	150
R-49	0.25	87	8×10^{-3}	-	120
R-50	0.25	87	10×10^{-3}	7×10^{-6}	180
Sphalerite crystal					
R-58	0.25	72	7.3×10^{-6}	-	960
R-59	0.25	57	3.1×10^{-6}	-	725
R-60	0.25	87	52.8×10^{-6}	-	605

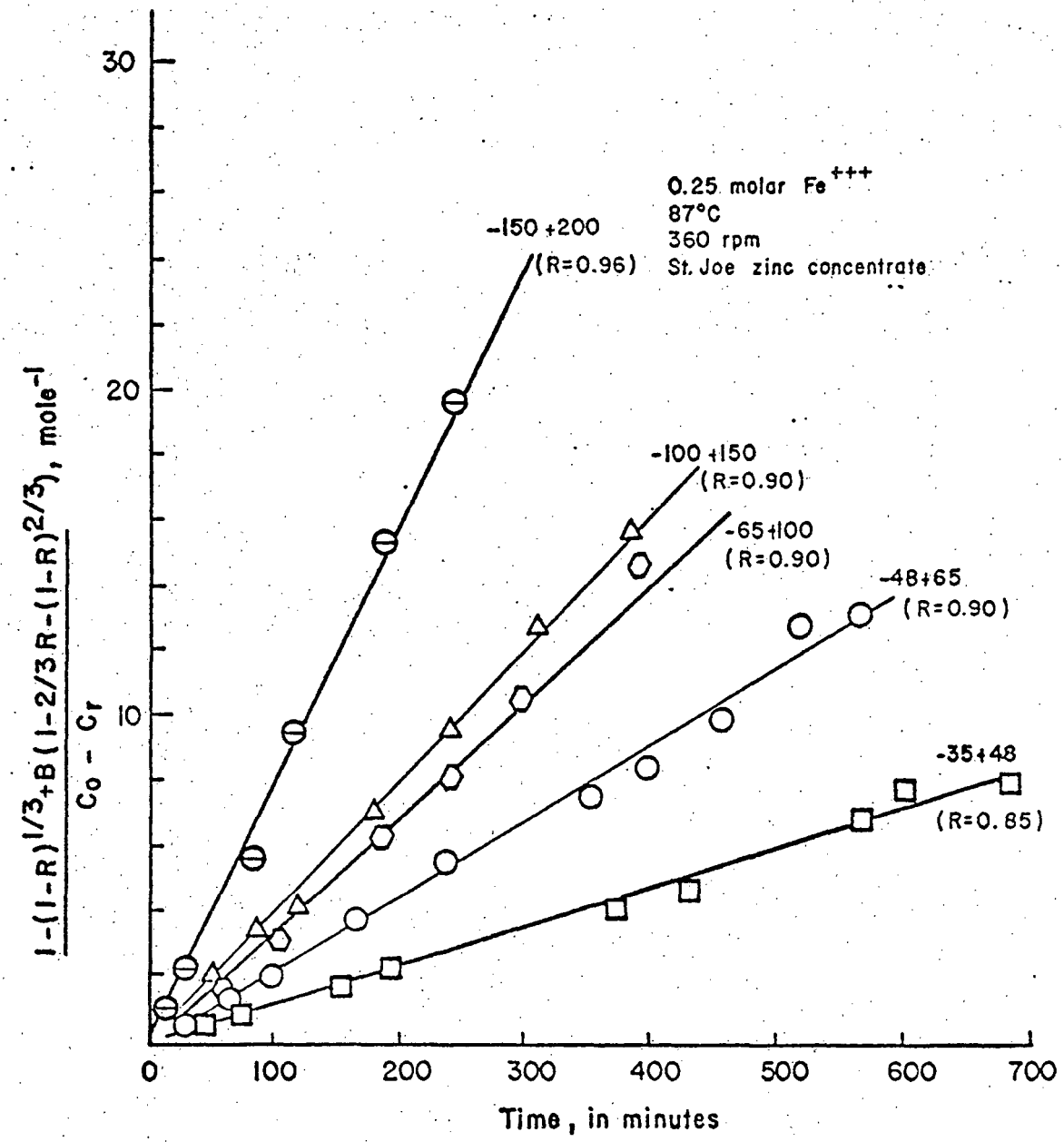

FIGURE 16.--EFFECT OF PARTICLE SIZE ON THE DISSOLUTION RATE.

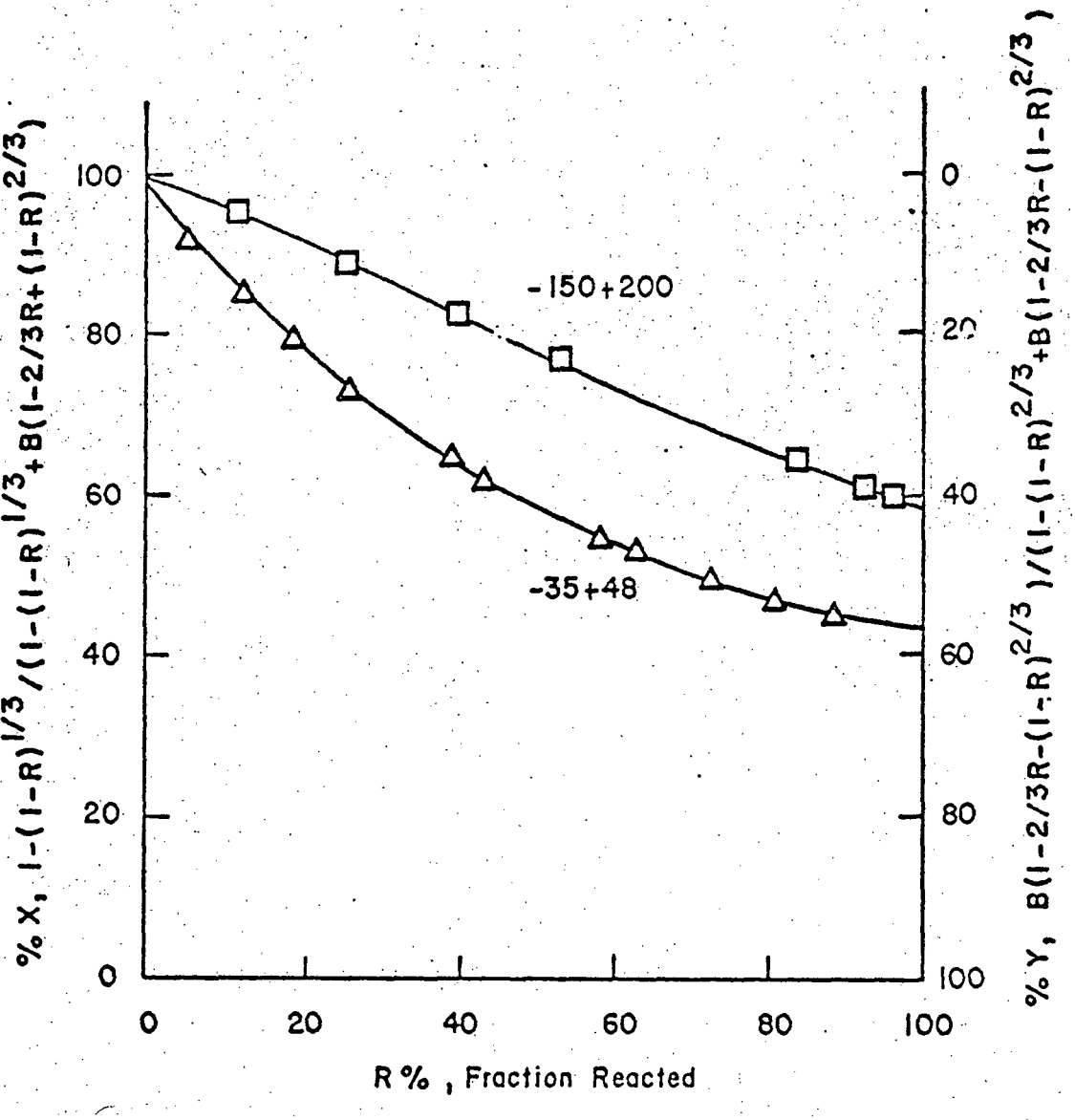

FIGURE 17.—DEPENDENCE OF CHEMICAL REACTION ON PARTICLE SIZE.

Table 8.--Effect of particle size on dissolution rate (0.25 molar Fe^{+++} ion, 87°C, 360 rpm, 5-gram sample from St. Joe Minerals)

Test No.	Particle Size (mesh)	Diameter r_o (cm)	Rate Constant K_{cc} ($cm.min^{-1}$)	Diffusion Coefficient D_e ($cm.min^{-1}$)	Dissolution Rate K_r ($min^{-1}.mole^{-1}$)	Constant B
			x 10^{-3}	x 10^{-5}	x 10^{-2}	
R-51	-28+35	0.02515	12.4	3.23	1.05	4.82
R-52	-35+48	0.01780	9.5	2.69	1.32	3.14
R-53	-48+65	0.01255	10.5	2.70	2.26	2.35
R-54	-65+100	0.00890	12.9	2.10	3.46	2.70
R-11	-100+150	0.00625	10.2	1.42	4.60	2.24
R-55	-150+200	0.00445	11.4	1.43	5.40	1.80
R-56	-150+200	0.00445	11.5	1.51	5.10	1.80

R. Figure 17 shows that the rate of dissolution of the smaller particle size (-150 + 200 mesh) is predominantly controlled by the reaction at the sulfur-sulfide interface while the larger particle -35 + 48 mesh is initially surface reaction controlled but approaches diffusional control in the later stages of leaching. It also indicates that for a given value of R the large particles give a greater diffusion resistance than chemical reaction resistance.

Effect Of Impurities

The dissolution rate can be influenced by the impurity content, through galvanic effects, or through catalytic effects. According to Romankiw and De Bruyn (1964), the more ionic in nature the Zn-S bond is, the more soluble the solid. Romankiw and De Bruyn compared the dissolution rate of pure zinc blende (ZnS) with that of an ore sample. One ore sample studied was marmatite (Zn,Fe)S in which the iron is more electropositive than zinc. It was found that the presence of iron in the lattice increased the ionic character of the crystal and aided in the dissolution.

In this study two samples of sphalerite were used to determine the effects of impurties. One was a bulk ore sample from St. Joe Minerals Company, Balmat, N.Y. The other was a piece of pure sphalerite crystal. The ore sample contained sphalerite, calcite, marmatite, quartz, pyrite, galena, and dolomite. The crystal was a pure zinc sulfide with no detectable impurities as determined by microprobe analysis. A comparison of the leaching curves of the two

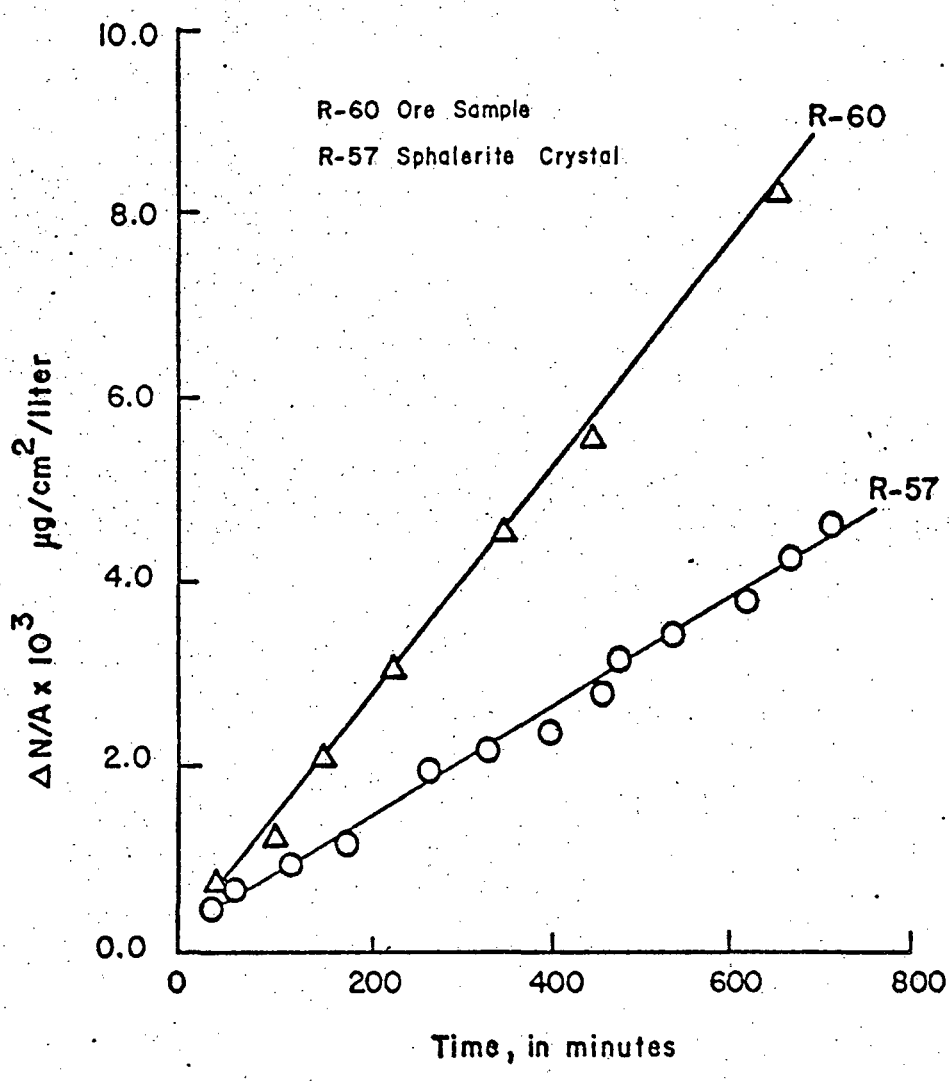

FIGURE 18.--DISSOLUTION RATE AS A FUNCTION OF CHEMICAL IMPURITIES.

materials (fig. 18) shows that the impure sample leaches at a faster rate than the pure sample. In addition to the marmatite contained in the impure sample, some MnS, which is an essentially ionic sulfide, was also present. Thus, the observed greater rate of dissolution of ore sample may be explained in part by the presence of ionic Fe and Mn in the sphalerite.

Increasing dissolution rates also result from galvanic effects (Hiskey and Wadsworth, 1974; Vizsolyi and others, 1963) and the catalytic role of the impurity (Scott and Dyson, 1968). Galvanic effects take place when a mixture of minerals are subjected to leaching in the same pulp, especially between electrically conducting minerals such as sulfides which leads to accelerated corrosion of some minerals and cathodic protection of others. For example, the rate of dissolution of sphalerite increases when sphalerite is in contact with pyrite (Hiskey and Wadsworth, 1974). The pyrite acts as a cathodic site for the reduction of oxygen that speeds the dissolution of sphalerite. An electrochemical type reaction was proposed as follows:

$$\text{Cathodic: } \tfrac{1}{2}\,O_2 + 2H^+ = 2e^- = H_2o \text{ (on pyrite)}$$

$$\text{Anodic : } ZnS = Zn^{++} + S^\circ + 2e^-$$

$$+$$

$$ZnS + \tfrac{1}{2}\,O_2 + H^+ = Zn^{++} + S^\circ + H_2O$$

Pyrite, as the cathode, carries a much larger current in the presence of oxygen than in the absence of oxygen.

Scott and Dyson (1968) reported that pure zinc sulfide is relatively inert under acidic, oxidizing, pressure leaching conditions. The zinc sulfide becomes activated and reacts rapidly to yield zinc sulfate and elemental sulfur when treated with soluble compounds of copper in small amount, and iron in larger amounts. The iron and copper play catalytic roles as cathodic sites in the ZnS anodic dissolution. Because the impure ore sample used in this part of the study contains iron and copper, they may be acting as catalysts and aiding the dissolution.

Empirical Rate Equation

The experimental data can be fitted to an empirical mathematical expression. Two such expressions have been tried--the logarithmic and hyperbolic equations. Regression analyses of these two equations were made by using the same experimental data obtained from the zinc concentrate leaching; fraction converted, R, vs reaction time, t. Comparing these two expressions, the data better fit the hyperbolic equation which has the correlation coefficient 0.996,

Table 9.--Constants in empirical rate equation

Hyperbola: $\frac{1}{R} = a + b\frac{1}{t}$
R: Fraction converted, %
t: Time, minutes
a & b: Constants
Stirring Speed, 360 rpm.

Test No.	Particle size (mesh)	Temperature (C°)	Fe^{+++} Concentration (molar)	Constants a	b
R-35	-100 + 150	44	0.25	1.066	559.05
R-51	-28 + 35	87	0.25	1.039	228.85
R-52	-35 + 48	87	0.25	0.844	241.97
R-53	-48 + 65	87	0.25	0.775	160.86
R-54	-65 + 100	87	0.25	0.765	101.89
R-11	-100 + 150	87	0.25	0.820	82.63
R-55	-150 + 200	87	0.25	0.750	60.46

and coefficient of determination 0.99 in the logarithmic expression, it is 0.968 and 0.94.

The general form of the hyperbolic equation is as follows (table 9):

$$\frac{1}{R} = a + \frac{b}{t} \qquad (13)$$

where R = fraction converted, %

t = time, minutes

a & b = constant

Rearranging, the rate equation will be

$$\text{Rate} = \frac{1}{t} = \frac{(1-aR)}{bR} \qquad (14)$$

From table 9 and Equation (14), the results indicate that the constants "a" and "b" vary directly with the particle diameter and inversely with temperature. This result is expected and is a consequence of the increased dissolution of smaller particles in a given period of time and the increase in reaction rate with temperature.

Analysis Of Error

Several sources of error can exist in any reaction rate study such as those arising from the reaction system and those involving the characteristics and operation of atomic absorption instruments. Errors from the reaction system are variations in temperature and agitation speed. Errors from the atomic

absorption analysis are variation in lamp current, interference, and stability of signal. There is always the human error associated with the reading of absorbance scales and the preparation of samples. Some errors are random and statistical, and some are systematic.

Random errors or accidental errors cannot be eliminated. They exist by the nature of measurements and appear to affect the precision of experimental results. The errors may vary with each atomic absorption determination or leaching experiment and are random, each contributing to a scattering of the data: (1) atomic absorption variation in instrument performance because of fluctuation of signals, (2) variation in burette and pipet reading because of temperature changes and human errors on reading the solution volume, (3) concentration variation in standard solutions, especially loss due to the absorption on the container wall while the solution stays inside a container for a certain period of time, and (4) volume variation in diluting the sample and in preparation of sample solutions.

Random error, revealed by small differences made from experiment to experiment, could be reduced or narrowed to a precise level by conducting a large number of experiments. However, conducting large numbers of experiments is too costly and laborious. During this investigation samplings and leaching experiments were duplicated to serve as a check and to increase the confidence in the reliability of the value obtained. Precautions and steps on duplicating the sampling from the reaction vessel, double checking the burette and pipette reading, and duplicating the standard solution analyses or renewing the standard solutions, would reduce the random error as much as possible. For zinc analysis the precision level 0.1 percent was obtained.

Systematic error is a determinate error which introduces a bias into the leaching experiment or into the atomic absorption analysis. They can be avoided once they are recognized. In atomic absorption analysis, systematic errors may be due to a faulty hollow-cathode lamp, matrix interference, and the detection limit of the instrument. In a reaction system they may be due to the reaction variables such as temperature and agitation speed.

When a lamp is failing, the most common effects are a reduction in analytical sensitivity and an increase in output fluctuation. Some effect occurs when the lamp is not warmed long enough, or when the lamp current is not set at the required level for that element of interest.

High concentrations of ferric chloride solution may cause the matrix interferences in atomic absorption analysis. When the sample solution becomes more concentrated and viscous, it flows more slowly through the burner, and atomic absorbance is decreased. The dilution of sample solutions and use of standard or blank solutions would help to overcome this interference problem.

Due to the detection limit of the instrument, zinc concentrations below 0.1 ppm may cause difficulty in reading absorption percentage on the recorder chart. However, there is no significant effect on results of sphalerite concentrate leaching experiments, because all these leaching solutions have zinc concentrations exceeding 0.1 ppm. When leaching for sphalerite crystal some errors on reading the recorder chart may occur due to the low value of zinc content in the leaching solution. Precision levels of 0.1 percent may be obtained by use of a digital readout of absorption.

The systematic errors could be minimized as much as possible in the reaction system by controlling the temperature and agitation speed. For an isothermal leaching experimentation, the temperature was controlled within $\pm$ 1°C by thermostat inside the oil bath. The expected error in rate constant, calculated from the differential form of the Arrhenius equation, $\frac{d\ln K_{cc}}{dT} = \frac{-E_A}{RT^2}$ or $\frac{\Delta K_{cc}}{Kcc} = \frac{-E_A}{RT} \cdot \frac{\Delta T}{T}$ was then 18 percent at 87°C with temperature error range $\pm$1.0°C. The results of early tests under seemingly identical conditions were of poor reproducibility. One fault was traced to the introduction of inert nitrogen gas into the vessel with a consequent error in rate constant; therefore, the nitrogen was turned off during the leaching period to ensure an isothermal reaction system.

It was assumed that during the leaching the solids are 100% suspended and no sulfur product layer abraded off the surface of the particles. But when using low agitation speed or large amounts of solid particles, all of the solid particles may not be suspended; thus causing the errors in reaction rate and interpretation of reaction model. Also, for certain high speed and long duration of agitation, the produced sulfur layer may be abraded off. This may change the reaction model from mixed kinetics to pure chemical kinetics throughout the leaching process. However, there was no experimentation in this aspect and the extent of errors was not determined in this study. The sample size was

limited to 5 grams of zinc concentrate in 500 milliliters of leaching solution and the agitation speed was controlled at 360±15 rpm. With such small ratio of solid-solution and moderate speed, very little sulfur was found abraded off the particles in the leaching experiments. As a result, the experimental results were found to follow the theoretical mixed-control model.

SUMMARY AND CONCLUSIONS

The major part of this study has concerned the kinetic model of sphalerite dissolution in acidified ferric chloride solution, and the evaluation of the variables such as temperature, particle size, ferric ion concentration, stirring rate, and purity. The following conclusions are drawn on the basis of the experimental results.

1. The rate of dissolution increases with stirring speed but there is a limiting stirring speed, 300 rpm, above which the reaction rate remains constant. The rate is controlled by chemical reaction at the sulfur-sulfide interface and by diffusion of ions through the sulfur layer above this speed, below the limiting speed the rate is controlled by diffusion of ions through the liquid layer around the particles.
2. Three sample sizes (5-gram, 1-gram, and 0.5-gram) of zinc concentrates were used in this study. Other conditions remained the same. The experimental data and the theoretical interpretation indicate that the process of dissolution is controlled by two steps. During the initial stages of leaching, the process is controlled predominantly by the rate of the reaction of ferric ion with the sulfide at the sulfur-sulfide interface. Transport of ions across the product sulfur layer was found to be important during the later stages of reaction. The mixed-kinetics equation is given by:

$$K_r t = [1 - (1-R)^{1/3}] + B[1 - \tfrac{2}{3}R - (1-R)^{2/3}]$$

where K_r = rate, min^{-1}
t = time, minutes
R = fraction converted, %
B = constant for mixed-control model

3. Reaction rate increases significantly with temperature. A calculation of the temperature dependence of the rate constant gives an activation energy of -11.2 Kcal per mole for sphalerite concentrate, which is in the range of values found by others.

4. For ferric iron concentration less than 0.1 molar the rate of dissolution may be controlled by absorption of ferric ions on the sulfide surface as a part of interface reaction. At higher ferric ion concentration, the rate of dissolution follows the mixed-kinetics model.

5. The presence of iron and manganese in the sphalerite apparently increases the rate of dissolution.

6. The experimental data fit an empirical rate equation of the form

$$\frac{1}{R} = a + \frac{b}{t}$$

where R = fraction reacted, %

a & b = constant

t = leaching time, minutes

7. A sulfur layer was evident on the surface of the sphalerite crystals as determined by electron beam microanalysis. Thickness of sulfur layer grew with increasing time of leaching.

8. Assuming pseudo-steady state conditions, diffusion coefficient for ions are about 10-16 x 10^{-6} cm^2/min at 87°C and rate constant, 10-16 x 10^{-3} cm/min at 87°C. Both are temperature dependent.

REFERENCES

Ablanov, A. D., and others, 1961, Treatment of ores of Nikolaevsk Deposit: Trudy Inst. Metall. Obegashch., Alma Ata, v. 3, 1960, p. 90-104, Chemical Abstracts, v. 55, 16309 p.

Bartlett, R. W., 1972, Pore diffusion-limited metallurgical extraction from ground ore particles: Metallurgical Transactions, AIME, v. 3, p. 913.

Beckstead, L. W., Munoz, P. B., Sepulveda, J. L., Herbst, J. A., Miller, J. D., Olson, F. A., and Wadsworth, M. E., 1976, Acid ferric sulfate leaching of attritor-ground chalcopyrite concentrates, in Extractive metallurgy of copper: AIME, v. 2, p. 611-617.

Bloss, F. Donald, 1971, Crystallography and crystal chemistry: Holt, Rinehart and Winston, Inc., p. 228, 545 p.

Brown, S. L. and Sullivan, J. D., 1934, Dissolution of various copper minerals: U.S. Bureau of Mines Report of Investigations 3228.

Carey, C. D., 1971, Ferric chloride leaching of a terahedrite concentrate: Master's thesis, University of Idaho.

Cordell, G. B., 1968, Reaction kinetics of the production of ammonium sulfate from anhydrite: Industrial and Engineering Chemistry Process Design and Development, v. 7, No. 2, pp. 278-284.

Dutrizac, J. E., and MacDonald, R. J. C., 1974, Ferric ion as a leaching medium, in Minerals Science and Engineering, v. 5, no. 2, p. 59-100.

Dutrizac, J. E.; MacDonald, R. J. C.; and Ingraham, T. R., 1969, The kinetics of dissolution of synthetic chalcopyrite in aqueous acidic ferric sulfate: Metallurgical Transactions, AIME, v. 245, p. 955.

Ermilov, V. V., 1961, Leaching sulfide concentrate with simultaneous dissolution of liberated free sulfur: Trudy Institute Met. I. Obogashcheniya, Akad. Nauk Kazakh. SSR3, 1960, p. 168-183, in Chemical Abstracts, v. 55, p. 16312.

Habashi, R., 1970, Principles of extractive metallurgy, v. 1: Gordon and Breach, p. 153-163, 413 p.

Haver, F. P., and Wong, M. M., 1971, Recovering elemental sulfur from nonferrous minerals, ferric chloride leaching of chalcopyrite concentrate: U.S. Bureau of Mines, Report of Investigations 7474.

Hiskey, J. B., and Wadsworth, M. E., 1974, Galvanic conversion of chalcopyrite: Solution Mining Symposium, AIME, Dallas, Texas, p. 422-445.

Jan, R. J., Hepworth, M. T., and Fox, V. G., 1976, A kinetic study on the pressure leaching of sphalerite, Metallurgical Transactions B. v. 7B, p. 353-361.

Jones, D. L., and Peters, E., 1976, The leaching of chalcopyrite with ferric sulfate and ferric chloride: International Symposium on Copper Extraction and Refining, Las Vegas, Nevada, 1055 p.

Kolthoff, I. M., Belcher, R., Stenger, V. A., and Matsuyama, G., 1957, Volumetric analysis: Interscience Publishers, Inc., New York, v. 3, p. 173-180, 724 p.

Kuzminkh, I. N., and Yakhontova, E. L., 1951, Action of ferric sulfate solutions on zinc sulfide, Zh. Priklad. Khim, v. 23, p 1121-1125, in Chemical Abstracts, v. 45, 1951, 1478 p.

Latimer, W. M., 1952, Oxidation potentials [2d ed.]: Prentice-Hall, Inc., p. 221-233, 352 p.

Levenspiel, Octave, 1972, Chemical reaction engineering [2d ed.]: John Wiley & Sons, Inc., New York, p. 357-377, 578 p.

Lowe, D. F., 1970, The kinetic of the dissolution reaction of copper and copper-ion: doctoral thesis, University of Arizona, p. 24.

Lu, Wei-Ko, 1963, The general rate equation for gas-solid reactions in metallurgical process: Metallurgical Transactions, AIME, V. 227, February, p. 203.

Murray, R. J., 1972, The dissolution of a galena concentrate in aqueous ferric chloride solution: doctoral thesis, University of Idaho.

Pohlman, S. L., and Olson, F. A., 1974, A kinetic study of acid leaching of chrysocolla using a weight loss technique: Solution Mining Symposium, AIME, Dallas, Texas, p. 447-459.

Pourbaix, Marcel, 1966, Atlas of electrochemical equilibria in aqueous solutions: Pergamon Press, p. 20-410.

Romankiw, L. T., and De Bruyn, P. L., 1964, Kinetics of dissolution of zinc sulfide in aqueous sulfuric acid-unit process in hydrometallurgy: Metallurgical Society Conferences, Gordon and Breach, v. 24, p. 45.

Scott, T. E., and Dyson, N. F., 1968, The catalyzed oxidation of zinc sulfide under acid pressure leaching conditions: Transactions AIME, v. 242, p. 1815.

Surana, V. S., and Warren, I. H., 1969, The leaching of geothite: Transactions, Institute of Mining and Metallurgy, p. 133-138.

Taylor, H. S., 1931, Chemical reaction at surfaces: Chemical Review, v. 9, no. 1, p. 1-45.

Tugov, N. I., and Tsyganov, G. A., 1965, Hydrometallurgical method for obtaining metallic antimony from concentrates: Industrial Chemical Engineering, v. 5, no. 1, p. 105.

Vizsolyi, A., Veltman, H., and Forward, F. A., 1963, Aqueous oxidation of galena under pressure in ammonia solution: Metallurgical Transaction, AIME, v. 227, p. 214.

Wadsworth, M. E., and Malouf, E. E., 1972(a), Theory and practice--First tutorial symposium on hydrometallurgy: University of Utah, p. 9-30.

_____, 1972(b), Theory and practice--Second tutorial symposium on hydrometallurgy, University of Utah, p. 10-45.

Wen, C. Y., 1968, Noncatalytic heterogeneous solid fluid reaction models: Industrial and Engineering Chemistry, v. 60, no. 9, p. 34-56.

Zapevalov, G. G., and Vygoda, R. M., 1964, Leaching of complex mattes with acid and ferric chloride solution: Trudy Irkutsk. Politek. Inst., v. 18, p. 92-99, in Chemical Abstracts, v. 61, 2768 p.

Calculation of Eh-pH Diagram of Sphalerite

1. $E^\circ = \Delta G_r^\circ / nf$

$\Delta G_r^\circ = \Delta G^\circ$ products $- \Delta G^\circ$ reactants

n = number of electrons transferred

f = 23.06 Kcal/volt equivalent

2. $Eh = E^\circ + \frac{RT}{nf} \ln \frac{\text{oxidized state}}{\text{reduced state}}$

$$= \frac{\Delta G_r^\circ}{nf} + \frac{RT}{nf} \ln \frac{\text{oxidized state}}{\text{reduced state}}$$

Eh = half cell potential relative to the standard hydrogen electrode

E° = standard half cell potential in volts; the volts of the half cell when the activities are unity for all species entering into the half reaction.

3. $\log K = - \frac{\Delta G_r^\circ}{2.303RT}$

ΔG_r° = standard free energy change for the reaction

K = equilibrium constant

R = 1.98 cal/mole deg

T = temperature in degree $^\circ K$

4. Reaction equations:

In these calculations the concentration of zinc ions in solution is assumed 0.05 mole and the summation of the concentration of the sulfur species in solution is assumed to be 0.05 mole. The concentration of iron ions is 0.25 mole which is the amount of ferric chloride in the solution.

(1) $2H_2O = O_2 + 4H^+ + 4e^-$

$$Eh = 1.23 + \frac{0.059}{4} \log [H^+]^4 [p_{O_2}]$$

Assume p_{O_2} = 1 atm

$$Eh = 1.23 - 0.059\ pH$$

(2) $H_2 = 2H^+ + 2e^-$

$$Eh = 0 + \frac{0.059}{2} \log [H^+]^2$$

$$= 0 - 0.059\ pH$$

(3) $Zns = Zn^{++} + S^o + 2e^-$

$E^o = 0.20$ volts

$Zn^{++} = 10^{-1.3}$

$$Eh = 0.20 + \frac{0.059}{2} \log Zn^{++}$$

$$= 0.20 + 0.0295 \times (-1.3) = 0.16\ v$$

(4) $HSO_4^-\ (aq) = H^+ + SO_4^{--}\ (aq)$

$$K = 10^{-1.19} = (SO_4)^{--} \frac{(H^+)}{HSO_4^-}$$

Assume $(SO_4^=) = (HSO_4^-)$

pH = 1.91

(5) $S^o\ (c) + 4H_2O = HSO_4^-\ (aq) + 7H^+ + 6e^-$

$HSO_4^- = 10^{-1.3}$ mole, $E^o = 0.338$ volts

$$Eh = 0.338 - 0.0688\ pH + \frac{0.059}{6} \log [HSO_4^-]$$

$$= 0.325 - 0.0688\ pH$$

(6) $S^{\circ}\ (c) + 4H_2O = SO_4^{--} + 8H^+ + 6e^-$

$E^{\circ} = 0.357$ volts, $SO_4^{--} = 10^{-1.3}$ mole

$Eh = 0.357 - 0.0788\ pH + 0.010 \log [SO_4^{--}]$

$= 0.344 - 0.0788\ pH$

(7) $HS^- + 4H_2O = SO_4^{=} + 9H^+ + 8e^-$

$E^{\circ} = 0.252$ v.

Assume $SO_4^{=} = HS^-$

$$Eh = 0.252 - 0.066\ pH + 0.0074 \log \frac{[SO_4^{--}]}{[HS^-]}$$

$= 0.252 - 0.066\ pH$

(8) $H_2S = S^{\circ}\ (c) + 2H^+\ 2e^-$

$E^{\circ} = 0.142$ v, $H_2S\ (aq) = 10^{-1.3}$ mole

$$Eh = 0.142 - 0.059\ pH + \frac{0.059}{2} \log \frac{1}{H_2S}$$

$= 0.18 - 0.059\ pH$

(9) $HS^- = S^{\circ} + H^+ + 2e^-$

$[HS^-] = 10^{-1.3}$ mole, $E^{\circ} = -0.065$

$Eh = -0.065 - 0.029\ pH - 0.029 \log [HS^-]$

$= -0.0273 - 0.029\ pH$

(10) $H_2S = H^+ + HS^-$

$$K = 10^{-7.0} = [H^+] \frac{[HS^-]}{H_2S\ (aq)}$$

Assume $[HS^-] = [H_2S]$

$pH = 7$

(11) $4H_2O + ZnS = Zn^{++} + SO_4^{--} + 8H^+ + 8e^-$

$E^o = 0.334$ v.

$Eh = 0.334 - 0.059\ pH + \frac{0.059}{8} \log Zn^{++}\ SO_4^{--}$

Assume $= Zn^{++} = SO_4^{--} = 10^{-1.3}$ mole

$Eh = 0.32 - 0.059\ pH$

(12) $ZnS + 6H_2O = Zn(OH)_2 + SO_4^{--} + 10H^+ + 8e^-$

$E^o = 0.426$ v $\quad SO_4^{--} = 10^{-1.3}$ mole

$Eh = 0.426 - 0.0738\ pH + 0.00738 \log [SO_4^{--}]$

$= 0.416 - 0.0738\ pH$

(13) $Zn^{++}(aq) + 2H_2O = Zn(OH)_2 + 2H^+$

$K = 10^{-11.8} = \frac{[H^+]^2}{Zn^{++}}$

Assume $Zn = 10^{-1.3}$ mole

$pH = 6.55$

(14) $Fe^{++} = Fe^{+++} + e^-$

$E^o = 0.771$ volts

$Eh = 0.771 + 0.0591 \log \frac{Fe^{+++}}{Fe^{++}}$

$= 0.771$ volts

(15) $Fe^{+++} + H_2O = FeOH^{++} + H^+$

Assume $FeOH^{++} = Fe^{+++}$

$\log \frac{[FeOH^{++}]}{[Fe^{++}]} = -2.43 + pH$

$pH = 2.43$

$(FeOH^{++} + H_2O - Fe_2O_3\ (s) + 4H^+)$

(16) $Fe^{++} + H_2O = FeOH^{++} + H^+ + e^-$

Assume $FeOH^{++} = Fe^{++}$

$$Eh = 0.914 - 0.0591\ pH + 0.0591 \log \frac{Fe(OH^{++})}{Fe^{++}}$$

$$= 0.914 - 0.0591\ pH$$

(17) $Fe^{++} + 2H_2O = HFeO_2^- + 3H^+$

$$\log \frac{HFeO_2^-}{Fe^{++}} = 31.58 + 3\ pH$$

$$pH = 10.6$$

(18) $Fe^{++} + 4H_2O = 8H^+ + FeO_4^{--} + 4e$

$$Eh = 1.462 - 0.1182\ pH + 0.0148 \log \frac{FeO_4^{--})}{Fe^{++}}$$

Assume $FeO_4^{--} = Fe^{++}$

$$Eh = 1.462 - 0.1182\ pH$$

(19) $HFeO_2^- + 2H_2O = FeO_4^{--} + 5H^+ + 4e^-$

$$Eh = 0.993 - 0.0739\ pH + 0.0148 \log \frac{FeO_4^{--})}{(FeO_2H^-)}$$

Assume $FeO_4^{--} = FeO_2H^-$

$$Eh = 0.993 - 0.0739\ pH$$

(20) $FeOH^{++} + 3H_2O = FeO_4^{--} + 7H^+ + 3e^-$

$$Eh = 1.652 - 0.1379\ pH + 0.0197 \log \frac{[FeO_4^{--})]}{(FeOH^{++})}$$

Assume $FeO_4^{--} = FeOH^{++}$

$$Eh = 1.652 - 0.1379\ pH$$

(21) $Cl^- + 4H_2O = ClO_4^- + 8H^+ + 8e^-$

$$Eh = 1.389 - 0.0591\ pH + 0.0074 \log \frac{ClO_4^-}{Cl^-}$$

Assume $ClO_4^- = Cl^-$

$Eh = 1.389 - 0.0591\ pH$